

1 Temporal variability of reactive iron over the Gulf of Alaska Shelf

2

3 Ana M. Aguilar-Islas^{a*}, Marie J.M. Séguret^a, Robert Rember^b, Kristen N. Buck^c, Peter Proctor^d,
4 Calvin W. Mordy^d, and Nancy B. Kachel^d

5

6 ^a School of Fisheries and Ocean Sciences, University of Alaska Fairbanks, PO Box 757220,
7 Fairbanks, AK 99775, USA

8 ^b International Arctic Research Center, University of Alaska Fairbanks, 930 Koyukuk,
9 Fairbanks, AK 99775, USA

10 ^cBermuda Institute of Ocean Sciences, St. George's GE01, BERMUDA; Present address:
11 College of Marine Science, University of South Florida, 140 7th Ave S,
12 St. Petersburg, FL 33701, USA

13 ^d Pacific Marine Environmental Laboratory, NOAA, 7600 Sand Point Way NE
14 Seattle, WA 98115, USA

15

16

17 * Corresponding author

18 Email: amaguilarislas@alaska.edu

19 Phone: 907 474 1524

20

21 Key words: iron, trace metals, Gulf of Alaska, Sub-Arctic Pacific, Seward Line, iron-binding
22 ligands

23

24

25

26 Deep Sea Research II. Special Edition Gulf of Alaska

1 **Abstract**

2
3
4
5
6
7
8
9
10
11
12
13
14
15
16
17
18
19
20
21
22
23
24
25
26
27
28
29
30
31

The Gulf of Alaska (GoA) shelf is a highly productive regime bordering the nitrate-rich, iron (Fe) limited waters of the central GoA. The exchange between nitrate-limited, Fe-replete coastal waters and nitrate-rich, Fe-deplete offshore waters, amplified by mesoscale eddies, is key to the productivity of the region. Previous summer field studies have observed the partitioning of Fe in the coastal GoA as being heavily dominated by the particulate phase due to the high suspended particulate loads carried by glacial rivers into these coastal waters. Here we present new physico-chemical iron data and nutrient data from the continental shelf of the GoA during spring and late summer, 2011. The late summer data along the Seward Line showed variable surface dissolved iron (DFe) concentrations (0.052 nM offshore to 4.87 nM inshore), within the range of previous observations. Relative to available surface nitrate, DFe was in excess (at Fe:C = 50 $\mu\text{mol}:\text{mol}$) inshore, and deficient (at Fe:C = 20 $\mu\text{mol}:\text{mol}$) offshore. Summer surface total dissolvable iron (TDFe, acidified unfiltered samples) was dominated by the acid-labile particulate fraction over the shelf (with a median contribution of only 3% by DFe), supporting previously observed Fe partitioning in the GoA. In contrast, our spring data from southeast GoA showed TDFe differently partitioned, with surface DFe (0.28 – 4.91 nM) accounting on average for a much higher fraction (~ 25%) of the TDFe pool. Spring surface DFe was insufficient relative to available nitrate over much of the surveyed region (at Fe:C = 50 $\mu\text{mol}:\text{mol}$). Organic Fe-binding ligand data reveal excess concentrations of ligands in both spring and summer, indicating incomplete titration by Fe. Excess concentrations of an especially strong-binding ligand class in spring surface waters may reflect *in-situ* ligand production. Due to anomalous spring conditions in 2011, river flow and phytoplankton biomass during our spring sampling were lower than the expected May average. We argue our samples are likely more representative of early spring pre-bloom conditions, providing an idea of the possible physico-chemical partitioning of Fe in coastal GoA waters relevant to initial spring bloom dynamics.

1 **1. Introduction**

2

3 The essential micro-nutrient iron (Fe) regulates primary productivity over large areas of the
4 open ocean including the Gulf of Alaska (GoA) high-nutrient, lower than expected chlorophyll
5 (HNLC) region (e.g. Martin et al., 1989; Boyd et al., 2004). Additionally, Fe availability
6 influences algal community composition, which transitions from a diatom-dominated community
7 at high concentrations of Fe to a system dominated by small phytoplankton at low Fe
8 concentrations (Morel et al., 1991; Landry et al., 1997). The biological regulatory effect of Fe
9 can also influence coastal waters (Hutchins et al., 1998; Johnson et al., 2001). As a consequence,
10 it is of interest to understand the factors that affect the distribution of biologically accessible Fe
11 in surface waters. Physical, chemical, and biological processes transform Fe in seawater by
12 altering its distribution within various pools, and thus its biological availability. Truly soluble (
13 $0.02 \mu\text{m}$) inorganic Fe, although it appears to be easily accessible to phytoplankton (Maldonado
14 and Price, 2000), is found at exceedingly low concentrations due to its extreme low solubility in
15 oxygenated seawater. Organic complexation increases the solubility of Fe in seawater (Liu and
16 Millero, 2002), and >99% of dissolved ($< 0.4 \mu\text{m}$) Fe (DFe) is organically complexed by strong
17 Fe-binding ligands that can allow for elevated DFe concentrations ([DFe]) (Buck et al., 2007;
18 Bundy et al., 2014). However, the biological availability of these complexes has been shown to
19 be variable (e.g. Maldonado and Price, 1999; Rijkenberg et al., 2006). In addition, a fraction of
20 the suspended particulate Fe pool may be mobilized into dissolved or soluble phases over short
21 time scales, rendering this labile fraction potentially available to phytoplankton (Johnson et al.,
22 1999). Together DFe and suspended labile particulate Fe represent reactive species that are
23 potentially significant to biological uptake.

24 Surface waters exhibit pronounced inshore-offshore gradients in DFe and suspended
25 particulate Fe, with inshore Fe concentrations enhanced by up to 2-3 orders of magnitude (or
26 greater), as has been observed in the GoA (Wu et al., 2009; Lippiat et al., 2010a). The gradients
27 result from the proximity of inshore waters to terrestrial Fe sources (aeolian, fluvial and
28 sedimentary). Atmospheric deposition, via episodic dust events from Asia and North America,
29 has been traditionally thought as the main mechanism for transporting Fe to the central GoA
30 (Boyd et al., 1998; Moore et al., 2002). Recent studies (Johnson et al., 2005, Lam et al., 2006,
31 Cullen et al., 2009; Lippiat et al., 2011; Brown et al., 2012) suggest fluxes of Fe from coastal

1 waters to the central GoA could be as important as atmospheric deposition. For example,
2 anticyclonic mesoscale eddies in the GoA that propagate from the inner shelf westward into the
3 basin (Ladd et al., 2005), are able to transport Fe-rich waters offshore (Johnson et al., 2005;
4 Lippiatt et al., 2011; Brown et al., 2012), and it has been calculated that the flux of reactive Fe
5 from mesoscale eddy activity in the GoA is in the same order of magnitude as atmospheric flux
6 (Brown et al., 2012). Lam et al. (2006) presented evidence of lateral advection of suspended
7 particulate Fe from the continental shelf into the remote HNLC region at depths of 0-300 m, and
8 Lam and Bishop (2008) calculated the flux of biologically available Fe to be within the same
9 order of magnitude for these two sources by assuming higher lability for sedimentary Fe as
10 compared to dust. Additional cross-shelf Fe transport via the California Undercurrent,
11 downwelling, and/or tidal currents could enhance the importance of coastal input relative to
12 atmospheric deposition, as suggested by Cullen et al. (2009).

13 Input of Fe to the GoA is highly seasonal. In the northern GoA prevailing winds stimulate
14 downwelling from fall through spring (Stabeno et al., 2004; Weingartner et al., 2005), and likely
15 contribute to episodic offshore flow of Fe in bottom layers. During May-October, weaker and
16 variable winds induce intermittent upwelling along the coast (Stabeno et al., 2004). Fresh water
17 runoff is at its peak between June and September, and higher concentrations of Fe have been
18 observed in July as compared to May in the inner GoA shelf (Wu et al., 2009). The various
19 glaciers along the mountainous GoA coastline cause rapid erosion and contribute to the high
20 suspended sediment (Christensen et al., 2000) and Fe loads (Lippiatt et al., 2010a) carried by
21 rivers. The rapid physical weathering of glaciers produces particles with a low labile Fe
22 component (Lippiatt et al., 2010a) as compared to more labile Fe-coatings on resuspended
23 particles that have been exposed to chemical reduction and re-oxidation processes at the
24 sediment-water interface (e.g. Hurst et al., 2010). Dust storms generated by episodic gap wind
25 events (Ladd and Chen, 2015; Ladd et al., 2015) can deposit glacial flour with high Fe loadings
26 (Crusius et al., 2011) over the shelf and offshore waters from exposed river beds of glacial rivers.
27 These events occur most frequently in mid-autumn (Ladd and Chen, 2015; Ladd et al., 2015)
28 when low river levels and snow cover expose the riverbed sediment (Crusius et al., 2011 and
29 references therein). The concentration of dissolved organic Fe-binding ligands likely caps the
30 amount of Fe from various inputs that contribute to the DFe pool, as observed in other river
31 influenced coastal systems (Buck et al., 2007), but inorganic colloidal Fe is potentially an

1 important component of the dissolved Fe pool in the high particle regime of the inner GoA shelf
2 during summer. Because most fluvial input of Fe is confined within the buoyancy driven Alaska
3 Coastal Current (ACC) (Figure 1), the ACC has the potential to act as Fe reservoir, and a vehicle
4 for alongshore transport (Wu et al., 2009).

5 We present Fe and ligand data from the continental shelf of southeast GoA during spring, and
6 the western GoA during late summer, 2011 (Figure 1), collected as part of the Gulf of Alaska
7 Integrated Ecosystem Research Program (GOA-IERP). Dissolved and particulate samples were
8 collected from surface waters and from depth profiles. Samples were processed to determine the
9 partitioning of Fe into various size classes and chemical species in order to show how the
10 physico-chemical speciation of Fe changes as a function of season and location in the Gulf of
11 Alaska, reflecting differences in Fe inputs. The various fractions of Fe discussed in this paper are
12 defined in Table 1. The study area borders the central HNLC GoA region and, considering the
13 recently described importance of cross-shelf processes in delivering Fe to the central GoA, the
14 seasonal partitioning of Fe over the shelf is likely important in determining the offshore flux of
15 biologically available Fe to the subarctic north Pacific.

16 17 **2. Materials and Methods**

18 19 **2.1. Sampling Region**

20
21 Observations were made in spring 2011 (30 April – 21 May) onboard the *R/V Thomas G.*
22 *Thompson* in the eastern GoA, and in late summer 2011 (14 – 20 September) onboard the *M/V*
23 *Tiglav* in the western GoA. During spring, seven transects were opportunistically sampled from
24 Chatham Strait to Kayak Island (Figure 1), and vertical profiles were collected from a subset of
25 GOA-IERP stations along three cross-shelf lines (South East Line A (SEA), South East Line G
26 (SEG), and Yakutat Bay Line C (YBC)) (Figure 1). Stations along the SEA line were sampled on
27 5 May, those along the SEG line were sampled twice (on 7 May and 17 May), and the YBC
28 stations were sampled on 11 May. In late summer, surface samples were collected along the
29 Seward Line on 16, 17, and 19 September, and in Prince William Sound on 15 September
30 (Figure 1).

31

1 2.2 Sampling Protocols

2

3 Sampling was conducted using trace-metal clean procedures recognized by the
4 International GEOTRACES Program ([http://www.geotraces.org/science/intercalibration/222-](http://www.geotraces.org/science/intercalibration/222-sampling-and-samplehandling-protocols-for-geotraces-cruises)
5 [sampling-and-samplehandling-protocols-for-geotraces-cruises](http://www.geotraces.org/science/intercalibration/222-sampling-and-samplehandling-protocols-for-geotraces-cruises)). Underway surface (~ 1 m)
6 sampling was accomplished using a towed trace metal clean pump system (Bruland et al., 2005;
7 Aguilar-Islas and Bruland, 2006). This system is composed of a PTFE diaphragm pump
8 (Wilden) and PFA Teflon™ tubing mounted onto a custom-made PVC vane which is attached to
9 a 20 kg PVC torpedo that hangs 1 m below the vane. The vane-torpedo assembly is deployed
10 from the side of the ship and towed away from the hull at speeds of 7-10 knots, depending on sea
11 conditions. Surface samples from the towed system were filtered in-line through a 0.2 µm pore
12 Supor Acropak 200 filter capsule (Pall Corporation) which was rinsed with at least 10 L of
13 seawater prior to use. Filtered and unfiltered samples for Fe analysis were collected into pre-
14 cleaned low density polyethylene (LDPE) bottles, acidified to pH ~1.8 (Optima grade HCl,
15 Fisher Scientific) (2 ml concentrated HCl/L) upon return to the laboratory, and analyzed after
16 one month of storage at room temperature. Filtered samples for Fe-binding organic ligands were
17 collected in fluorinated polyethylene acid-cleaned bottles and stored at -20 °C until analysis
18 (Buck et al., 2012). Filtered samples for macro-nutrient determination were collected in 60 mL
19 acid washed, high-density polyethylene bottles after three rinses. Samples were frozen (-20 °C)
20 and shipped to the laboratory for analysis.

21 Depth profiles for Fe were collected using University of Alaska Fairbanks (UAF) vanes (Wu
22 2007, Wu et al., 2009). UAF vanes are a modified version of the Moored In-Situ Trace Element
23 Serial Sampler (MITESS, Bell et al., 2002) consisting of a single MITESS module attached to a
24 2-L polyethylene square bottle. The assembly was mounted onto a plastic vane that was attached
25 to the ship's hydrowire. The bottom-most vane was positioned 10 m above the ship's rosette
26 system. The MITESS modules were programmed to open/close bottles simultaneously after
27 bottles sat for at least 10 minutes at the target depths. During sample collection, the vane portion
28 of the assembly positions the sampling bottle upstream of the hydrowire, allowing for the
29 collection of uncontaminated seawater samples. Upon retrieval, the 2L bottles were stored in the
30 refrigerator until processed (0-6hrs). Seawater was vacuum-filtered through acid-cleaned 47 mm
31 diameter 0.4 µm track-etched polycarbonate membranes (Nuclepore, Whatman), and the filtrate

1 was collected in the same bottle types as for surface samples. The membranes were folded into
2 eighths, placed into pre-cleaned 7 mL polypropylene vials and stored at -20 °C. Blank filter
3 membranes were treated in the same manner as samples, but using Milli-Q water (18.2 MΩ cm)
4 instead of seawater.

5 Sample processing during spring (*R/V Thompson*) was carried out within a plastic
6 enclosure under HEPA filtered air (ISO Class 5) in the ship's main laboratory. During late
7 summer (*M/V Tiglax*), due to on-board laboratory space limitations, depth profiles were not
8 collected and surface in-line unfiltered and filtered samples were collected under plastic bells on
9 the deck of the ship, taking care to avoid contamination. Plastic bells were made with lidded
10 plastic containers outfitted with a bulkhead tubing connector to interface with the tubing coming
11 from the surface pump system into the inside of the container. The plastic container was large
12 enough to accommodate maneuverability during sampling. The lidded end of the bell was kept
13 closed in between samplings. Two bells were constructed, one for filtered and the other for
14 unfiltered sample collection. Table 2 summarizes sampling operations during 2011.

15 Conductivity, temperature and depth (CTD) data for profiles on the *R/V Thomas G.*
16 *Thompson*, were obtained from a SeaBird SBE 911 plus CTD sensor within a 24-bottle rosette
17 system, chlorophyll fluorescence from a WetLabs ECO chlorophyll fluorometer with factory
18 calibration, and light transmission was measured with a Wet Labs CSTAR Transmissometer.
19 Underway salinity, temperature, and fluorescence data was obtained from the underway system
20 of the *R/V Thomas G. Thompson* during spring. The fluorometer for the underway system was
21 not calibrated at sea; therefore, the raw data represents a relative measure of chlorophyll
22 fluorescence levels at the surface. During late summer on the *M/V Tiglax*, underway salinity and
23 temperature were obtained from a Midi Hydro-Bios MultiNet equipped with a Hydro-Bios CT-
24 Set sensor. The towed trace metal clean pump system was deployed (recovered) immediately
25 after (before) MultiNet recovery (deployment), and the obtained temperature and salinity were
26 from within 500 m from the sample collected for Fe analyses.

27

28 2.3. Suspended Particle Processing

29

30 Filters containing suspended particulate samples were thawed, leached and digested upon
31 return to the laboratory. Optima grade acids (Fisher Scientific) were employed during leach and

1 digestion protocols. A modified leach technique based on the one described by Berger et al.,
2 (2008) was employed. Thawed folded filters were kept in their 7 mL vials, and 1 mL of 25 %
3 acetic acid with 0.02 M hydroxylamine hydrochloride ($\text{NH}_2\text{OH} \cdot \text{HCl}$) was added to each vial.
4 The vials were then placed in a water bath, heated to 90-95 °C for 10 min, and left to cool
5 gradually down to 30 °C for the duration of the 2 h leach. The heating step releases intracellular
6 Fe while the reducing agent accesses the portion of Fe associated with oxyhydroxide coatings
7 (Berger et al., 2008). Leachates were transferred into 10 mL PTFE beakers (Jensen Inert
8 Products) and heated to near dryness. After the beakers cooled, 100 μL of 1 M HNO_3 was added
9 and heated. The solution was transferred into acid-clean 7 mL polyethylene vials by rinsing the
10 beaker 3 times with 1 M HNO_3 (1 mL per rinse) and the solution was stored until analysis at
11 room temperature. Each leached folded filter was transferred to a 15 mL Teflon vial (Savillex
12 Corp.) and a 4-step digestion, modified from Morton et al., (2013), was carried out: 1) 1 mL of
13 concentrated HNO_3 was added and allowed to reflux for 12 h at 130 °C, then the solution was
14 taken down to near dryness; 2) a mixture of concentrated HNO_3 (1 mL), concentrated HCl (500
15 μL) and concentrated HF (100 μL) was added and allowed to reflux for 12 h at 130 °C, then
16 taken down to near dryness; 3) concentrated HNO_3 (1 mL) and HCl (500 μL) were added and
17 left to reflux for 12 h at 130 °C, then taken down to near dryness; 4) 1 mL of concentrated HNO_3
18 was added and refluxed for 30 min at 130 °C. Once cooled, the digested solution was transferred
19 to a LDPE 30 mL bottle, and the vial was rinsed 4 times with 0.1% HNO_3 to yield a final 5%
20 HNO_3 solution. Blank filters were leached and digested in the same manner as samples. Blanks
21 for the leaching ($0.70 \text{ ppb} \pm 0.1 \text{ ppb}$ ($n = 7$)) and digestion ($0.25 \text{ ppb} \pm 0.07 \text{ ppb}$ ($n = 8$))
22 procedures represented 0 – 13% and 1 – 29% of the samples, respectively.

23

24 2.4. Analytical methods

25

26 2.4.1. Iron determination

27

28 Analyses were carried out at the University of Alaska Fairbanks on an Element 2 (Thermo-
29 Finnigan) inductively couple plasma mass spectrometer. Seawater DFe and TDFe were
30 quantified by isotope dilution with high resolution inductively coupled plasma mass
31 spectrometry (HR-ICP-MS) detection after $\text{Mg}(\text{OH})_2$ co-precipitation (Wu and Boyle 1998).

1 Briefly, 1.6 mL of filtered seawater sample and the isotope spike are mixed in a 2 mL vial
2 followed by the addition of ammonium hydroxide. The vial is then centrifuged, the supernatant is
3 decanted, and the precipitate is diluted in 4% HNO₃ (Optima grade, Fisher Scientific).
4 Procedural blanks were determined using 50 µl of seawater with a known low (<0.1 nM) [DFe]
5 and were on average 0.05 nM (n = 8), and the detection limit (3σ) was 6 pM. Accuracy was
6 determined from the analysis of the reference sample SAFE D2 (0.923 ± 0.008 nM; n = 13)
7 which was within the latest community consensus value (SAFE D2 = 0.933 ± 0.023 nmol/kg)
8 reported in May, 2013 (www.geotraces.org). Suspended LPFe and RPF_e were determined by
9 direct injection into the mass spectrometer as described by Aguilar-Islas et al., (2013) using a
10 calibration curve and Ga as an internal standard. Values are reported as nmol of Fe per L of
11 filtered seawater (nM).

12

13 2.4.2. Organic Fe-binding ligand determination

14

15 Dissolved Fe-binding ligand concentrations and conditional stability constants were determined
16 by competitive ligand exchange-adsorptive cathodic stripping voltammetry (CLE-ACSV) with
17 the added competitive ligand salicylaldoxime (Rue and Bruland, 1995; Buck et al., 2007; 2012).
18 Frozen seawater samples were thawed at room temperature, shaken, and distributed into 12
19 Teflon lidded vials (Savillex) in 10 mL aliquots. A borate-ammonium buffer was used to
20 maintain pH of 8.2 (NBS; Ellwood and van den Berg, 2001) in all vials. Dissolved Fe additions
21 employed in the titrations were +0, 0, 0.25, 0.5, 0.75, 1, 1.5, 2, 2.5, 3.5, 5, 7.5 nM. Following
22 two or more hours of equilibration between the dissolved Fe additions and natural ligands in the
23 sample, 25 µM of the competitive ligand salicylaldoxime (SA) was added to each vial and the
24 resulting Fe-SA complex was then determined by ACSV on a BASi controlled growth mercury
25 electrode (Buck et al., 2007; 2012). Resulting titration data were interpreted using a combination
26 of van den Berg/Ruzic and Scatchard linearization approaches, and reported results represent the
27 average outputs from the two linearizations (Buck et al., 2007; 2012). Up to two ligand classes
28 were determined from each individual titration, while the notation for a given sample's ligand
29 classes was defined by the conditional stability constant determined for each class: Ligands with
30 $\log K_{FeL_i, Fe}^{cond} > 12$ are defined as L₁, L₂ for $\log K_{FeL_i, Fe}^{cond} = 11 - 12$, and L₃ for $\log K_{FeL_i, Fe}^{cond} = 10 - 11$
31 (Gledhill and Buck, 2012).

1
2
3
4
5
6
7
8
9
10
11
12
13
14
15
16
17
18
19
20
21
22
23
24
25
26
27
28
29
30
31

2.4.3. Macro-nutrient determination

Concentrations of nitrate, nitrite, ammonium, phosphate and silicic acid were determined using a combination of analytical components from Alpkem, Perstorp and Technicon. The WOCE-JGOFS standardization and analysis procedures specified by Gordon et al. (1994) were closely followed including reagent preparation, calibration of labware, preparation of primary and secondary standards, and corrections for blanks and refractive index. Concentrations of secondary standards were verified using commercial standards from OSIL.

2.4.4 Iron Fractions

Four operationally defined Fe species were measured: 1) Dissolved Fe (DFe) is the filtered fraction of iron that passes through the inline 0.2 μm filter capsule (tow fish) or the 0.4 μm filter membrane (UAF vanes); 2) Total dissolvable Fe (TDFe) is the fraction of iron obtained from unfiltered samples acidified to pH \sim 1.8. This was only obtained from tow fish samples; the particulate Fe fraction (retained by the 0.4 μm filter membrane) was obtained from vertical profile samples, and 3) Leachable particulate Fe (LPFe) is the fraction of particulate Fe solubilized by an acetic acid leach; while 4) Refractory particulate Fe (RPFe) is the strong acid digested particulate Fe fraction. Based on these measured species, three calculated fractions were obtained: 1) Particulate Fe is the sum of LPFe and RPFe; 2) Acid-labile particulate Fe (ALPFe) is the fraction of particulate Fe that dissolves when an unfiltered sample is acidified to pH 1.8 (TDFe – DFe); and 3) Reactive Fe is the fraction that is kinetically reactive and potentially available to biology in short timescales of days to weeks, defined by Lippiat et al., (2010a) as DFe + LPFe, and here also defined by TDFe. When referring to “labile particulate Fe” we include both ALPFe and LPFe fractions. These definitions of various Fe fractions are summarized in Table 1.

3. Results

The upwelling index (NOAA Bakun Index) for the region indicated downwelling-favorable winds over most of both sampling periods, with short episodes of relaxation and weakly

1 upwelling winds during both seasons. As expected, river discharge during our spring sampling
2 was low, with an average daily discharge for the Alsek and Copper rivers of 376 m³/sec and 837
3 m³/sec, respectively, as compared to the average daily 2011 peak discharge flow in July and
4 August of 2237 m³/sec for the Alsek River and 4546 m³/sec for the Copper River (USGS
5 surface-water daily statistics data, 2011). However, river discharge during our spring sampling
6 was also ~ 1/3 lower relative to the same sampling period in previous years (2004-2010; 573
7 m³/sec for the Alsek River and 1232 m³/sec for the Copper River) (available USGS surface-
8 water daily statistics data). This lower discharge was in part related to the delay in the onset of
9 the spring freshet in 2011 (USGS surface-water daily statistics data) as compared to previous
10 years (2004-2010; data not shown).

11 Relative to climatological May values (Waite and Mueter, 2013), the biomass present during
12 our May 2011 sampling was anomalously low (Strom and Fredrickson, 2015), and this
13 anomalously low production persisted throughout the spring of 2011 (Stabeno et al., 2015). The
14 phytoplankton community in May 2011 is described by Strom and Fredrickson (2015) as
15 consisting mainly of picophytoplankton (< 2 µm) cells that exhibited low specific growth rates
16 and acclimation to low light conditions.

17

18 3.1 Spring Surface Transects

19

20 Temperature (T), salinity (S), nitrate plus nitrite (N+N), fluorescence, DFe and TDFe along
21 transects are presented in Figures 2a-f. Surface T ranged from ~ 6 °C to 9 °C with the lowest T
22 values near shore in the vicinity of Chatham Strait and Cross Sound. Higher salinity Alaska Gyre
23 water (S = 32.6-32.8, Musgrave et al., 1992) was not encountered during spring. Sampled surface
24 waters ranged in S from 30.95 to 32.25 with the lowest near Yakutat Bay and Kayak Island, and
25 the highest offshore of Cross Sound and Yakutat Bay. In general the concentration of N+N had
26 not been depleted, and concentration ranged from 0.18 to 12.27 µM (Figure 2d). Samples with
27 low N+N (< 1 µM) were collected in the vicinity of Cross Sound and Kayak Island. Chlorophyll
28 fluorescence values from the underway sensor varied from ~ 0.02 to 0.2V, with a narrow area of
29 higher values in late May near Chatham Strait. In situ Chl *a* and satellite data (Strom and
30 Fredrickson, 2015; Stabeno et al., 2015; Waite and Mueter, 2013) indicated an anomalously low
31 spring bloom during 2011, especially in the eastern GoA. The concentration of DFe was on

1 average 1.52 ± 1.04 nM, and ranged from 0.28 to 4.91 nM. The highest concentrations were
2 observed near Cross Sound and Kayak Island, and the lowest concentrations were observed
3 offshore. There was no clear trend for DFe over the narrow salinity range sampled, although the
4 freshest water collected ($S = 30.95$) had an elevated [DFe] of 4.50 nM, and the lowest surface
5 DFe (0.28 nM) was measured in offshore higher salinity water ($S = 32.11$). The concentration of
6 TDFe ranged over nearly 3 orders of magnitude, from 0.72 to 260 nM, with a median value of
7 4.73 nM and a few samples near Cross Sound, Yakutat Bay, and Kayak Island containing TDFe
8 in excess of 100 nM. The partitioning of TDFe between ALPFe and DFe was highly variable,
9 with DFe accounting for ~ 1.5% to 80% of the TDFe pool (~25% on average) over the sampled
10 area.

11 A subset of spring surface samples analyzed for dissolved Fe-binding organic ligands showed
12 two ligand classes (stronger (L_1) and relatively weaker (L_2)) present in all samples (Table 3). The
13 L_1 -type ligands had high conditional stability constants ($\log K_{FeL_1,Fe}^{cond} = 12.2 \pm 0.17$ to 13.0 ± 0.05 ;
14 Table 3) and L_1 concentrations were in excess of DFe, dominating the ligand pool. The
15 conditional stability constants for L_1 in the spring surface samples were the highest of any
16 samples analyzed in this Gulf of Alaska dataset (Table 3).

17

18 3.2 Spring Depth Profiles

19

20 Vertical profiles of T, S, DFe, beam transmission (Beam c), Chl a, LPFe and RPFfe for
21 Stations along the SEA, SEG and YBC lines are shown in Figures 3-6. In general, DFe, LPFe
22 and RPFfe exhibited similar trends with depth (Figures 7a-f).

23 Data from the SEA line are shown in Figure 3a-d. Station SEA20 (1011 m depth) is ~25 km
24 offshore from SEA5 (145 m depth). Within the surface mixed layer, waters were slightly warmer
25 and saltier at SEA20 (7.1 °C, $S \sim 32.1$) as compared to SEA5 (6.7 °C, $S \sim 31.9$) and Fe
26 decreased from inshore to offshore from ~ 1 nM DFe, ~ 2.6 nM LPFe, and ~ 6 nM RPFfe at
27 SEA5 to ~ 0.5nM DFe, ~0.6 nM LPFe, and ~ 2 nM RPFfe at SEA20. At Station SEA5, the
28 concentration of all Fe fractions increased with depth (2.39 nM DFe, 5.87 nM LPFe, and 15.6
29 nM RPFfe) to roughly twice their surface value. Increases with depth at SEA20 resulted in
30 maximum concentrations of 2.58 nM LPFe, and 9.81 nM RPFfe at 750 m. The maximum DFe at
31 SEA20 was 1.70 nM at 500m, decreasing to 1.17 nM at 750 m. An increase in light attenuation

1 (decrease in % Beam c) was observed at around 150 – 350 m, suggesting advection of sediment
2 from the shelf. At these stations DFe accounted for ~ 17% to 50% of the reactive Fe pool.

3 Data from stations along the SEG line are presented in Figures 4a-d (first occupation) and 5a-
4 d (second occupation). Water depth at Stations SEG0 and SEG20 were 110 m and 1700 m,
5 respectively. These stations are ~38 km apart. Due to time constraints SEG20 was only profiled
6 down to 360 m on the second occupation. The surface mixed layer at Station SEG0 had shoaled,
7 warmed and freshened on the second occupation (Figures 4a and 5a), and exhibited an order of
8 magnitude increase in Chl. The higher biomass in this fresher surface layer was likely advected
9 from inshore, as the large increase in Chl values were not apparent at Station SEG20 (Figures 4b
10 and 5b). At Station SEG20 salinity increased within the upper 250 m on the second occupation
11 suggest advection of offshore water or upwelling. At Station SEG0 LPFe and RPF_e were low (~1
12 to 4 nM RPF_e and 0.4 to 1.8 nM LPFe) and increased gradually with depth during both sampling
13 periods. The concentration of DFe also tended to increase with depth and ranged from 0.5 to 1.3
14 nM. Offshore, at SEG20 DFe had a similar concentration range (0.5 to 1.17 nM) with the higher
15 values at and below 200 m. Similar to SEA20, an increase in light attenuation was also observed
16 at around 150 to 350 m, but the change was gradual during the second occupation. The
17 concentrations of LPFe and RPF_e were higher offshore than over the shelf (SEG0), and ranged
18 from 0.6 to 3.6 nM for LPFe and from ~ 2 to 11 nM for RPF_e. The concentration of DFe
19 accounted for ~ 20% to 70% of the reactive Fe at these stations.

20 Data from Stations YBC10, YBC40 and YBC50+ are presented on Figures 6a-f. The shelf
21 widens in this region and YBC10 (165m depth) is ~ 55 km inshore of YBC40 (190m depth),
22 which is ~ 30 km inshore of YBC50+ (1400 m depth). The surface mixed layer was slightly
23 cooler and saltier offshore (7.0 °C, S ~ 32.4) as compared to the inshore station (7.4 °C, S ~32.1).
24 A bottom nepheloid layer was apparent from the reduction in % Beam c at Station YBC10 and to
25 a lesser extent at YBC40. An increase in light attenuation was also apparent from 50 to 100 m at
26 YBC 40 without a concomitant increase in Chl values. Similar to offshore stations SEA20 and
27 SEG20, Station YBC50+ exhibited an increase in light attenuation from 150 to 350 m. The
28 concentration of DFe at these stations tended to increase with depth. At YBC10 Fe was relatively
29 homogeneous ranging from 0.65 nM to 0.83 nM in DFe, from 0.38 nM to 0.77 nM in LPFe, and
30 with RPF_e at ~ 1 nM throughout the water column (nepheloid layer not sampled). Surface Fe
31 concentrations at Station YBC40 were similar to YBC10, and increased to 2.12 nM DFe, 18.9

1 nM LPFe, and 48.8 nM RPF_e at 75 m, where light attenuation increased. AT YBC 50+, DFe
2 exhibited a minimum concentration of 0.30 nM at 50 m, within a tongue of colder (5.5 °C) and
3 higher salinity (32.5) water compared to the surface mixed layer, and had a maximum of 1.65
4 nM at 300 and 500m, decreasing to 1.24 nM at 1000 m. Here the concentrations of LPFe and
5 RPF_e were highest at the surface (4.89 nM and 79.0 nM, respectively), lowest also at 50 m (0.79
6 nM and 3.54 nM, respectively), and increased in concentration at 300 m (2.16 nM and 12. 2nM,
7 respectively) within the area where light attenuation was enhanced. The concentration of DFe
8 accounted for ~ 10% to 60% of the reactive Fe at these stations.

9 Two classes of organic Fe-binding ligands were determined in most samples collected at 20
10 m, though only one ligand class was present at SEA20 and YBC50+. Ligands in the 20 m spring
11 samples were generally weaker, with lower conditional stability constants, than measured in
12 spring surface (1 m) waters (Table 3). In these 20 m samples, the ligands determined were
13 classified across three ligand classes based on conditional stability constants (Table 3), though
14 even the stronger L₁-type ligands were on the low end of conditional stability constants for this
15 ligand class ($\log K_{FeL_1,Fe}^{cond} = 12.04 - 12.15$) compared to those measured within the mixed layer
16 along surface transects (Table 3; 12.16 – 13.0).

17

18 3.3 Summer Surface Transects

19

20 Surface temperature along the Seward Line was relatively warm and homogeneous, ranging
21 from 10.4 °C to 11.0 °C (Figure 8a). In Prince William Sound, T was slightly warmer (11.4 °C),
22 and S was the freshest measured during the cruise (S = 24.9) (data not shown). Over the
23 continental shelf, salinity ranged from 26.1 at GAK 1 to 32.6 at GAK 13 (Figure 8b).
24 Temperature and salinity were not obtained on 16 September when the MultiNet was not
25 deployed. Daily variability in N+N, DFe, and TDFe (Figures 7a-c) was observed along the
26 Seward Line on re-occupied stations (GAK 4 – 7). The concentration of N+N from GAK 1 to
27 GAK 12 ranged between ~ 2 and 4 μM on 17 and 19 September, and was elevated (9.92 μM) at
28 the furthest offshore station, GAK 13 (Figure 8a), where Alaska Gyre water was sampled. Earlier
29 (16 Sep), higher concentrations of N+N (~ 6-7 μM) were observed from GAK 4 to GAK 5.5,

1 but similar concentrations of ~ 4 μM were observed from GAK 6 to GAK 7.5 (Figure 8a). In
2 Prince William Sound N+N was depleted (0.33 μM) (data not shown).

3 The concentration of DFe ranged by two orders of magnitude from 0.052 nM at GAK 13 to
4 4.87 nM at GAK 1 (Figure 8b), and correlated to salinity, with higher DFe at lower salinity
5 values. Subnanomolar [DFe] were observed from GAK 4 to GAK 7.5 on 16 September, and
6 from GAK 5 to GAK 13 on 17 and 19 September (Figure 8b). The concentration of TDFe varied
7 by three orders of magnitude from 0.19 nM at GAK 13 to 585 nM at GAK1 (Figure 8c). From
8 GAK 1 to GAK 12, TDFe was dominated by the ALPFe fraction, which was indicated by the
9 low percentage and relatively uniform (~ 1- 8%) fraction of DFe observed (Figure 8c). This
10 fraction increased to ~ 28% at GAK 13, where TDFe was found at subnanomolar concentrations.

11 Two classes of Fe-binding organic ligands were also determined in summer surface samples,
12 except at GAK 9, where one ligand class was observed. As seen in the spring samples, the two
13 ligand classes observed fit the definitions of three ligand classes based on conditional stability
14 constants, though the stronger L₁-type ligands observed in summer presented intermediate
15 conditional stability constants ($\log K_{FeL_1,Fe}^{cond} = 12.0 - 12.4$) to those measured between the surface
16 and 20 m during spring (Table 3) in southeast Alaska.

17

18 **4. Discussion**

19

20 4.1 Seasonal and spatial variability in reactive iron

21

22 Reactive Fe, the sum of DFe and the labile fraction of suspended particles, constitutes the
23 pool of Fe that is potentially available for biological uptake. Field and laboratory studies (e.g.
24 Chase et al., 2005; Hurst and Bruland, 2007; Rich and Morel, 1990) have shown that a fraction
25 of particulate Fe can be readily solubilized and become available for biological uptake on the
26 time scale of days. Given that in the Gulf of Alaska coastal rivers provide a massive input of
27 particulate material (0.3-0.45 km³/yr; Menard, 1979), and roughly one third of the mountainous
28 coastline here is irregularly covered by glaciers (Wang et al., 2004), glacially derived sediment is
29 likely the major source of reactive Fe to the coastal GoA (Lippiatt et al., 2010a). However, this
30 input is highly seasonal. The seasonal transport of sediment by coastal rivers peaks in late
31 summer/early autumn (Milliman and Syvitski, 1992) when fresh water discharge is at its

1 maximum from snow melt and summer rains (Weingartner et al., 2005). Additional glacial
2 sediment input can happen from mid to late autumn, along both the southeast and western GoA
3 regions, during episodic gap wind events that promote dust storms when anomalous northerly
4 winds provide sufficient energy to lift and transport sediment from exposed glacial river beds
5 (Ladd and Chen, 2015; Ladd et al., 2015; Crusius et al., 2011). Glacially derived sediment is
6 produced by physical weathering, and in coastal waters of the GoA, glacially derived suspended
7 particles have been shown to contain on average a lower percentage of LPFe (11% of suspended
8 particulate Fe) as compared to suspended sediment from coastal waters influenced by watersheds
9 where chemical weathering dominates (e.g. Columbia River plume with 26% LPFe) (Lippiatt et
10 al., 2010b). Although glacially-derived suspended particles contain less labile Fe, the massive
11 input of particulate material along the GoA coast can result in highly elevated LPFe and [TDFe]
12 that reach micromolar (μM) levels in low salinity river plumes (Lippiatt et al., 2010a; Schroth et
13 al., 2014). As a result, the relative contribution of DFe to the reactive Fe pool is smallest during
14 late summer, not only in coastal areas influenced by large glacial rivers such as the Copper and
15 Alsek rivers, but also in regions with smaller glacial river drainage. For example, during the late
16 summer of 2011, we observed highly elevated concentrations of ALPFe (580 nM) along the
17 Seward line in lower salinity (26.1) inshore water, and in surface shelf/shelf break waters along
18 this transect the contribution of DFe (< 5 nM) to the reactive pool had a median of only $\sim 3\%$
19 (Figure 8) in the late summer of 2011.

20 In contrast to the dominant contribution of particulate Fe to the reactive Fe pool observed in
21 late summer, the partitioning of Fe showed different characteristics during spring 2011. Spring
22 sampling took place in the absence of large riverine particulate input (low river flow conditions)
23 and at a time when biomass was anomalously low (Strom and Fredrickson, 2015; Stabeno et al.,
24 2015). Elevated ALPFe (> 100 nM) was sampled at the surface only in the vicinity of Yakutat
25 Bay and Kayak Island (Figure 2e-f), where the shelf broadens and glacial input becomes more
26 prevalent, but the median [ALPFe] was 4.5 nM. Station samples from 20 m depth contained
27 relatively low concentrations of LPFe (~ 19 nM or less; median 1.06 nM). Although the fraction
28 of the suspended particulate Fe that was leachable varied (6-42% LPFe), on average ($\sim 25\%$) it
29 was more akin to the average % LPFe found in suspended sediment of waters influenced by the
30 Columbia River plume (Lippiatt et al., 2010b). The contribution of DFe to the reactive Fe pool
31 tended to be greater during spring 2011 as compared to the late summer, with an average of 24%

1 in surface transects (1 m) and 41% in station profiles (20 m). Figure 9 shows DFe as a function
2 of reactive Fe concentrations. Within the lower range of reactive Fe values ($\sim 1 - 50$ nM), the
3 concentration of DFe tended to be higher during the spring than during late summer in 2011.
4 Also, data collected during the late summer of 2007 (Lippiatt et al., 2010a) was shifted towards
5 higher reactive Fe concentrations, but similar DFe as seen in spring 2011 (Figure 9). The
6 difference in the partitioning of reactive Fe observed between the two seasons is likely driven by
7 a combination of differences in river discharge and biological uptake histories leading to the time
8 of sampling. Nutrients were available (Figures 2d) in surface waters during spring 2011, and the
9 low biomass observed was the result of a delayed and greatly reduced spring bloom (Strom and
10 Fredrickson, 2015; Stabeno et al., 2015; Waite and Mueter, 2013), suggesting that biological
11 uptake had not yet depleted the DFe pool accumulated from the previous winter. Alternatively,
12 the differences in Fe partitioning observed during the two sampling seasons in 2011 could reflect
13 geographical differences, as our spring sampling locations were mainly south of the outflow of
14 larger rivers such as the Alsek and Copper rivers (Figure 1). Data from late summer 2007
15 (Lippiatt et al. 2010a) also point to geographical differences in reactive Fe partitioning between
16 the southeast GoA and the Seward Line, supporting the notion that differences in reactive Fe
17 observed in 2011 might reflect geographical, in addition to temporal differences (Figure 9).

18 Due to the conditions encountered, the partitioning of reactive Fe observed during May 2011
19 is likely more representative of that found during early spring in the southeast GoA, when river
20 runoff and the spring bloom have yet to get underway. In late winter, when prevailing winds
21 stimulate downwelling (Stabeno et al., 2004; Weingartner et al., 2005), and fluvial and aeolian
22 (Crusius et al., 2011) inputs are essentially absent, the main mechanism by which reactive Fe is
23 supplied to the surface is deep mixing by storms. The mixed DFe is expected to persist into
24 spring more readily than resuspended sedimentary particulate Fe. Thus, conditions leading into
25 the spring bloom in the Gulf of Alaska are likely characterized by a reactive Fe pool with a more
26 dominant DFe contribution. Similarly, coastal water entrained into the ubiquitous mesoscale
27 eddies of the GoA at the time of their formation over the southeast GoA shelf, which takes place
28 during late winter/early spring (Crawford, 2002; Ladd et al., 2007; Henson and Thomas, 2008),
29 is expected to have a reactive Fe pool not heavily dominated by labile particulate Fe.

30
31

1 4.2 The fate of the glacial Fe input

2

3 Glacial input of iron into the Gulf of Alaska varies greatly with season, with the majority of
4 the input taking place during summer via fluvial input, although during fall episodic offshore
5 flowing gap wind events (Ladd and Chen, 2015; Ladd et al., 2015) can bring glacial dust to the
6 Gulf of Alaska via atmospheric deposition. The bulk of the riverine input is trapped within the
7 buoyancy driven ACC, and freshwater plumes rich in dissolved and particulate Fe greatly reduce
8 their Fe load as they mix with coastal waters, which tend to carry similar concentrations of DFe
9 in late summer (Lippiatt et al., 2010a, and this study) as in spring (this study). The availability of
10 dissolved Fe-binding ligands likely caps the concentration of DFe as suggested by Lippiatt et al.
11 (2010a) and observed during this study. Sharp, non-conservative decreases in Fe concentrations
12 (of several orders of magnitude) across salinity gradients have been observed in late summer
13 along southeast and northern coastal Alaska (Wu et al., 2009; Lippiatt et al., 2010a; Schroth et
14 al., 2014) that indicate the rapid loss of dissolved and suspended Fe loads from freshwater
15 plumes along the coastally trapped ACC. Yet, even after rapid and substantial removal, the
16 enhanced input of glacial sediment in late summer results in labile particulate Fe
17 disproportionately contributing to and augmenting the reactive Fe pool of the summer ACC. The
18 summer ACC represents a reservoir of reactive Fe and provides a vehicle for alongshore
19 transport of Fe (Wu et al., 2009). The fate of the bulk of the glacially-derived iron is to be
20 deposited to the sediment, where it will be subsequently subjected to sedimentary transformation,
21 and could ultimately contribute to the transport of Fe from the shelf to the interior via
22 mechanisms of subsurface lateral advection (Lam et al., 2006; Cullen et al., 2009). Data from our
23 vertical profiles support the idea that suspended particles from the shelf could be laterally
24 transported offshore contributing Fe to the subsurface. Bottom nepheloid layers were observed at
25 the wider shelf stations YBC10 and YBC40 (Fig. 6a-d), and at station YBC50+ the reduction in
26 Beam c at ~150-250 m (Fig. 6f) suggest particles advection at these intermediate depths.
27 Although the differences in Beam c at these depths compared to 50 m immediately above and
28 below are small, the difference is statistically significant (Mann-Whitney Rank Sum Test; $P <$
29 0.001). Particle advection is less apparent at stations SEA20 and SEG20 where the shelf is quite
30 narrow. However, Beam c data at intermediate depths are significantly different than those from
31 layers immediately above and below.

1
2
3
4
5
6
7
8
9
10
11
12
13
14
15
16
17
18
19
20
21
22
23
24
25
26
27
28
29
30

4.3 Iron-binding Organic Ligands and DFe

The correlation between DFe and the reactive Fe fraction tends to be variable and non-linear (e.g. Figure 9, and Aguilar-Islas et al., 2013), and although Fe can exchange between the labile particulate and dissolved phases at seasonal and shorter timescales, the amount of DFe in seawater has been shown to rarely exceed the concentration of the strong Fe(III)-binding organic ligand class (L₁-type) (Buck et al., 2007; Biller et al., 2013). For the fresh-water plumes of the coastal GoA, Lippiatt et al. (2010a) speculated that low DOC in glacial melt water (Hood and Scott, 2008) results in low concentrations of L₁-type ligands, and that the low availability of excess ligands caps [DFe] in summer plumes leading to the observed lower than expected [DFe] relative to the highly elevated labile particulate Fe present in the system. We measured the concentration of dissolved Fe(III)-binding organic ligands during this study, and found that the concentrations of the stronger L₁-type ligands were in excess of DFe in all surface and subsurface spring, as well as in summer surface samples where an L₁ ligand class was identified (Table 3; Figure 10). This finding supports the notion that the availability of strong Fe(III)-binding organic ligands provides an upper bound for the concentration of DFe (Buck et al., 2007), and indicates that in GoA coastal waters L₁-type ligands are not necessarily fully titrated by Fe. The concentration of L₁-type ligands does seem to cap the contribution of DFe to the reactive Fe pool (Figure 10), and in absence of a greatly enhanced L₁-type ligand pool during late summer when particulate riverine input is high, the labile particulate fraction will tend to become disproportionately dominant.

During both spring and summer 2011 DFe was strongly bound in surface waters. Conditional stability constants provide a measure of the binding strength of a given ligand class with respect to inorganic Fe (Fe'), and we observed particularly high values of $\log K_{FeL_1,Fe'}^{cond}$ (Table 3) in spring surface samples. These high conditional stability constants are consistent with values determined for siderophores (Rue and Bruland, 1995; Buck et al., 2007; 2010), which are especially strong iron-binding ligands produced by bacteria for iron acquisition. They are also as high or higher than the conditional stability constants determined for unknown ligands produced by ambient biological communities in austral winter Southern Ocean coastal waters exposed to

1 spring light and temperature conditions (Buck et al., 2010). Thus, the higher $\log K_{FeL_1, Fe}^{cond}$ values
2 observed here, together with L_1 concentrations in excess of DFe are consistent with biological
3 ligand production in surface waters of the Gulf of Alaska during spring 2011. As previously
4 mentioned, spring 2011 had an anomalously reduced spring bloom (Stabeno et al., 2015), with
5 the phytoplankton community at the time of sampling consisting of low-light adapted cells
6 dominated by picophytoplankton ($\leq 2 \mu\text{m}$ cells) (Strom and Fredrickson, 2015). Although our
7 sampling took place in May, the characteristics of the Fe-binding ligand pool we observed in the
8 spring of 2011 may be more akin to the ligand pool found in coastal GoA waters during early
9 spring prior to the onset of the spring bloom.

10

11 4.4 Biological implications

12

13 Diatom blooms contribute significantly to the productivity of the GoA in coastal and offshore
14 waters (Strom et al., 2006; Peterson and Harrison, 2012). The ability of diatoms to adjust their
15 cellular Fe requirements and rapidly respond to changing available Fe concentrations plays a role
16 in their success. Diatoms can either lower their cellular Fe quotas as available Fe concentrations
17 become extremely low (e.g. McKay et al., 1997), or they can perform “luxury uptake” under
18 conditions of high bioavailable Fe concentrations (Sunda and Huntsman 1995). Based on Fe
19 availability, intracellular Fe:C ratios vary widely in diatoms, with coastal species requiring
20 higher ratios than their oceanic counterparts (Sunda and Huntsman, 1995; Bruland et al., 2001;
21 Marchetti et al., 2006). Field and laboratory studies (e.g. Bruland et al., 2001; Sunda and
22 Huntsman, 1995; Marchetti et al., 2006) have shown Fe:C ratios in non-Fe limited coastal
23 diatoms can vary from about 20 $\mu\text{mol Fe: mol C}$ at subnanomolar available Fe concentrations, to
24 approximately 50 $\mu\text{mol: mol}$ at $\sim 1 \text{ nM}$ available Fe, to over 100 $\mu\text{mol: mol}$ at available Fe
25 concentrations $\geq 3 \text{ nM}$. Although DFe is quantitatively chelated by organic Fe-binding ligands,
26 DFe provides a good measure of the Fe that is available to the phytoplankton community in time
27 scales of days (Bruland et al., 2001). Algal Fe requirements are also affected by light availability.
28 Low-light acclimation by phytoplankton requires an increase in Fe compounds involved in
29 photosynthesis (Falkowski et al., 1981), and because most intracellular Fe is used in these
30 compounds (Raven 1988), low-light acclimated phytoplankton, including diatoms, are

1 particularly susceptible to Fe availability. Even when diatom growth rates are depressed by light-
2 limitation, diffusion allows for maximum Fe uptake rates, but due to their larger cell size as
3 compared to oceanic species, coastal diatoms will experience diffusion limitation at [DFe] of a
4 few tenths of a nanomolar (Sunda and Huntsman, 1995). During our spring survey, surface DFe
5 (0.28 nM – 4.91 nM) had a median concentration of 1.25 nM. These concentrations are well
6 above concentrations likely to result in diffusion limitation for coastal diatoms, and in the range of
7 values for possible Fe “luxury uptake” by diatoms.

8 It is of interest to consider the macro- and micro-nutrient relationship of surface waters just
9 prior to the onset of the spring bloom in the GoA. Winter mixing brings high concentrations of
10 macronutrients into surface waters. Yet, due to particle scavenging of DFe, [DFe] mixed into the
11 surface are potentially not sufficient relative to nitrate concentrations, especially in the absence
12 of external DFe sources such as fluvial input. The conditions we encounter during May 2011
13 (low biomass and low-light adapted community dominated by picophytoplankton (Strom and
14 Fredrickson, 2015), reduced fresh water input conditions that suggest minor fluvial Fe input
15 (USGS river flow data), and relatively high surface [N+N]) are more akin to early spring
16 conditions, prior to the onset of the phytoplankton bloom, and we suggest early bloom nutrient
17 dynamics can be investigated using this data set.

18 Here our spring nutrient data is used to investigate whether DFe was sufficient relative to
19 available nitrate to support a coastal diatom bloom during early spring in the absence of
20 additional DFe input from fluvial or other sources. During May 2011, the [N+N] varied over two
21 orders of magnitude (0.18 -12.27 μM) and had a median concentration of 8.04 μM . The excess
22 Fe ($\text{Fe}_{(\text{ex})}$) relative to N+N is calculated in terms of cellular Fe:C ratios.

$$23 \quad \text{Fe}_{(\text{ex})} = [\text{DFe}] - ([\text{N+N}] \times \text{C:N} \times \text{Fe:C} / 1000)$$

24 Where the ratio of Fe:C is dependent on *in-situ* [DFe], and the units for [DFe] are nM, while
25 the units of [N+N] are μM . Given ambient [DFe] at this time (median = 1.25 nM), an Fe:C ratio
26 of $\sim 50 \mu\text{mol}:\text{mol}$ would be an appropriate estimate for the Fe requirement of coastal diatoms
27 over the GoA shelf during spring 2011. We calculate $\text{Fe}_{(\text{ex})}$ (Table 4) using this ratio, and a C:N
28 Redfield ratio of 106:16. Our small surface data set suggests that, in the absence of additional Fe
29 inputs, a spring bloom of coastal diatoms would eventually run out of Fe (negative $\text{Fe}_{(\text{ex})}$) over
30 most of the southeast shelf prior to becoming nitrate limited. Yet, the coastal GoA becomes
31 limited by nitrate as the growing season progresses (Childers et al., 2005), indicating other

1 nutrients (including Fe) are found in excess of nitrate. As shown by previous late summer
2 observations, surface [DFe] can remain relatively elevated (~ 2 nM) in surface waters of coastal
3 southeast Alaska when nitrate concentrations are depleted (Lippiat et al., 2010a). This
4 underscores the importance in the timing of external DFe delivery from fluvial (or other)
5 sources, and its along-shelf transport to the productivity of the coastal GoA. Suspended particles
6 from glacial rivers carry a reservoir of reactive Fe that can be readily mobilized into the
7 dissolved phase as needed throughout the growing season. Interestingly, although the median
8 surface [DFe] (1.25 nM) in May 2011 was not indicative of Fe limitation, other parameters
9 discussed above suggest a potential role for Fe in the productivity of spring 2011. Namely, the
10 pool of the of strong L₁-class Fe-binding ligand being consistent with *in-situ* production (Section
11 4.3), and the relatively high availability of N+N in surface waters along with the low diatom
12 abundance and low biomass (Stabeno et al., 2015; Strom and Fredrickson, 2015).

13 Summer DFe data (Wu et al., 2009; Lippiatt et al., 2010a; this study) along the Seward Line
14 show variable [DFe] as a function of surface salinity (Figure 11) that likely result from a
15 combination of inter-annual differences in biological uptake and the source of the surface water
16 traversing the region. In late summer 2011, surface offshore waters along the Seward Line
17 exhibited low [DFe] that were deficient relative to available nitrate (even when considering a
18 lower Fe:C of 20 $\mu\text{mol}:\text{mol}$, appropriate given the subnanomolar DFe concentraions) (Table 4).
19 The Seward Line is located in an area highly impacted by the trajectory of Yakutat eddies (Ladd
20 et al., 2007; Januot et al., 2009). The presence/absence of eddies and associated “streamers”
21 (Januot et al., 2009) likely contribute to the inter-annual variability of macronutrient and [DFe]
22 over the outer shelf and slope. Although variable, DFe appears to reach exceedingly low
23 concentrations of only a few tenths of a nanomolar or lower when surface salinity is > 32 (Figure
24 11). In this outer shelf/slope region, where we observed deficient [DFe], coastal diatoms may
25 experience diffusion limitation as [DFe] fall below a few tenths of a nanomolar. Thus, when
26 higher salinity water (>32) from the oceanic GoA meanders over the shelf, the very low [DFe]
27 likely limit diatom production, and contribute to interannual biomass variability observed along
28 the Seward line.

29

30 **5. Conclusions**

1 Prior to the large riverine discharge that is received by the coastal GoA during summer, the
2 partitioning of reactive Fe over the southeast GoA shelf was in contrast to that described for late
3 summer (Lippiatt et al., 2010), and was characterized by suspended particles with higher %LPFe
4 and a reactive Fe pool with a larger contribution by DFe as compared to previous summer
5 observations. Two classes of organic Fe-binding ligands were observed, with the stronger Fe-
6 binding classes (L_1 , L_2) found in excess of DFe. Excess L_1 concentrations with especially high
7 Fe-binding constants may suggest *in-situ* ligand production by an ambient biological community
8 stressed by Fe availability at the surface in spring 2011.

9 Due to the reduced river discharge and biomass concentrations encountered during May
10 2011, our spring samples are likely more representative of late winter/early spring pre-bloom
11 conditions over the shelf. Nutrient characteristics of GoA waters prior to the growing season
12 have implications for interannual variation in productivity. Our samples provide a look at the
13 possible physico-chemical partitioning of Fe and its relation to macronutrients relevant for eddy
14 source waters and the initiation of the bloom. A better understanding of the magnitude of nutrient
15 fluxes and the mechanisms involved in nutrient dynamics over the GoA is needed.

16 17 **Acknowledgements**

18 We thank the captain and crew of the *R/V Thomas G. Thompson* and the *M/V Tiglax* for their
19 kind assistance during cruise operations. We thank Phyllis Stabeno and Russell Hopcroft for ship
20 time contributions, Dave Kachel for his support during the deployment and recovery of UAF
21 vanes onboard the *R/V Thomas G. Thompson*, and Dean Stockwell for assistance during
22 sampling onboard the *M/V Tiglax*. We also thank three anonymous reviewers for insightful
23 suggestions that improved this manuscript. This work was funded by grants from the North
24 Pacific Research Board to Ana M. Aguilar-Islas (G84/F4185-00) and to Calvin Mordy
25 (G83/F5183-01) as part of the Gulf of Alaska Integrated Ecosystem Research Project, and
26 supported by NOAA's Ecosystems & Fisheries-Oceanography Coordinated Investigations
27 (EcoFOCI) program. This publication was partially funded by the Joint Institute for the Study of
28 the Atmosphere and Ocean (JISAO) under NOAA Cooperative Agreement NA10OAR4320148,
29 and is contribution EcoFOCI-0814 to EcoFOCI, contribution 2380 to JISAO, contribution 4114
30 to NOAA's Pacific Marine Environmental Laboratory, and GOAIERP publication number **XX**.

1 Kristen N. Buck was supported by institutional funding from the Walwyn Hughes Fund for
2 Innovation and the Ray Moore Endowment Fund at the Bermuda Institute of Ocean Sciences
3 (BIOS). The findings and conclusions in this paper are those of the authors and do not
4 necessarily represent the views of NOAA's Oceans and Atmospheric Research.

5

1 **References**

- 2 Aguilar-Islas, A. M., Rember, R., Nishino, S., Kikuchi, T., and Itoh, M., 2013. Partitioning and
3 lateral transport of iron in the Canada Basin. *Polar Sci.*, doi:10.1016/j.polar.2012.11.001.
- 4 Aguilar-Islas, A.M. and Bruland, K.W., 2006. Dissolved manganese and silicic acid in the
5 Columbia River plume: A major source to the California Current and coastal waters off
6 Washington and Oregon. *Mar. Chem.* 101, 233-247.
- 7 Bell, J., Betts, J., and Boyle, E., 2002. MITESS: a moored in situ trace element serial sampler for
8 deep-sea moorings. *Deep-Sea Res. I* 49, 2103-2118.
- 9 Berger, C.J.M., Lippiatt, S.M., Lawrence, M.G., Bruland, K.W., 2008. Application of a chemical
10 leach technique for estimating labile particulate aluminum, iron, and manganese in the Columbia
11 River plume and coastal waters off Oregon and Washington. *J. Geophys. Res.-Oceans* 113,
12 C00B01.
- 13 Biller, D.V., Coale, T.H., Till, R.C., Smith, G.J., Bruland, K.W., 2013. Coastal iron and nitrate
14 distributions during the spring and summer upwelling season in the central California Current
15 upwelling regime. *Cont. Shelf Res.* 66, 58-72
- 16 Boyd, P.W., Wong, C.S., Merrill, J., et al., 1998. Atmospheric iron supply and enhanced vertical
17 carbon flux in the NE subarctic Pacific: Is there a connection? *Global Biogeochem. Cycles* 12,
18 429-441.
- 19 Boyd, P.W., Law, C.S., Wong, C.S., Nojiri, Y., Tsuda, A., Levasseur, M., Takeda, S., Rivkin, R.,
20 Harrison, P.J., Strzepek, R., Gower, J., McKay, R.M., Abraham, E., Arychuk, M., Barwell-
21 Clarke, J., Crawford, W., Crawford, D., Hale, M., Harada, K., Johnson, K., Kiyosawa, H., Kudo,
22 I., Marchetti, A., Miller, W., Needoba, J., Nishioka, J., Ogawa, H., Page, J., Robert, M., Saito,
23 H., Sastri, A., Sherry, N., Soutar, T., Sutherland, N., Taira, Y., Whitney, F., Wong, S.E.,
24 Yoshimura, T., 2004. The decline and fate of an iron-induced subarctic phytoplankton bloom.
25 *Nature* 428, 549-553.
- 26 Brown, M. T., Lippiatt, S. M., Lohan, M. C., et al., 2012. Trace metal distributions within a Sitka
27 eddy in the northern Gulf of Alaska. *Limnol. Oceanogr.* 57, 503-518.
- 28
- 29 Bruland, K. W., Rue, E. L., Smith, G. J., 2001. The influence of iron and macronutrients in coastal
30 upwelling regimes off central California: implications for extensive blooms of large diatoms.
31 *Limnol. Oceanogr.* 46, 1661–1674.
- 32
- 33 Bruland, K.W., Rue, E.L., Smith, G.J., DiTullio, G.R., 2005. Iron, macronutrients and diatom
34 blooms in the Peru upwelling regime: brown and blue waters of Peru. *Mar. Chem.* 93, 81–103.
- 35 Buck, K. N., M. C. Lohan, C. J. M. Berger, and K. W. Bruland. 2007. Dissolved iron speciation
36 in two distinct river plumes and an estuary: Implications for riverine iron supply. *Limnol.*
37 *Oceanogr.* 52, 843-855.
- 38 Buck, K.N., Lohan, M.C., Berger, C.J.M., Bruland, K.W., 2007. Dissolved iron speciation in two
39 distinct river plumes and an estuary: Implications for riverine iron supply. *Limnol. Oceanogr.*, 52,
40 843-855.

- 1 Buck, K. N., J. Moffett, J., K. A. Barbeau, K.A., et al., 2012. The organic complexation of iron
2 and copper: an intercomparison of competitive ligand exchange-adsorptive cathodic stripping
3 voltammetry (CLE-ACSV) techniques *Limnol. Oceanogr.-Methods* 10, 496-515
- 4 Buck, K.N., Selph, K.E., Barbeau, K.A., 2010. Iron-binding ligand production and copper
5 speciation in an incubation experiment of Antarctic Peninsula shelf waters from the Bransfield
6 Strait, Southern Ocean. *Mar. Chem.* 122, 148-159.
- 7
- 8 Bundy, R., D.V. Biller, K.N. Buck, K.W. Bruland, and K.A. Barbeau, 2014. Distinct pools of
9 dissolved iron-binding ligands in the surface and benthic boundary layer of the California Current.
10 *Limnology and Oceanography*, 59, 769-787.
- 11
- 12 Chase, Z., Hales, B., Cowles, T., Schwartz, R., van Geen, A., 2005. Distribution and variability of
13 iron input to Oregon coastal waters during the upwelling season. *Journal of Geophysical Research-*
14 *Oceans* 110, C10S12.
- 15 Childers, A.R., Whitley, T.E., Stockwell, D.A., 2005. Seasonal and interannual variability in
16 the distribution of nutrients and chlorophyll a across the Gulf of Alaska shelf: 1998-2000. *Deep-*
17 *Sea Res. II* 52, 193-216.
- 18 Christensen, H.H., Mastrantonio, L., Gordon, J.C., Bormann, B.T., 2000. Alaska's Copper River:
19 humankind in a changing world. United States Department of Agriculture, General Technical
20 Report, PNW-GTR-480, 20 p.
- 21 Crawford, W.R., 2002. Physical characteristics of Haida eddies. *J. Oceanogr.* 58, 703-713.
- 22 Crusius, J., Schroth, A. W., Santiago, G. et al., 2011. Glacial flour dust storms in the Gulf of
23 Alaska: Hydrologic and meteorological controls and their importance as a source of bioavailable
24 iron. *Geophys. Res. Lett.* 38, 10.1029/2010GL046573
- 25 Cullen, J. T., Chong, M., Ianson, D., 2009. British Columbian continental shelf as a source of
26 dissolved iron to the subarctic northeast Pacific Ocean. *Global Biogeochem. Cycles* 23, GB4012
- 27 Elmwood, M.J., van der Berg, C.M.G., 2001. Determination of organic complexation of cobalt in
28 seawater by cathodic stripping voltammetry. *Mar. Chem* 75, 33-47.
- 29
- 30 Falkowski, P.G., Owens, T.G., Ley, A.C., Mauzerall, D.C., 1981. Effects of growth irradiance
31 levels on the ratio of reaction centers in two species of marine phytoplankton. *Plant Physiology*,
32 68, 969-973
- 33
- 34 Gledhill, M., Buck, K.N., 2012. The organic complexation of iron in the marine environment: A
35 review. *Front. in Microbiol.: Microbiolog. Chem.* 3, Article 69.
- 36 Gordon, L.I., J. C. Jennings Jr., A. A. Ross, J. M. Krest (1994). A suggested protocol for
37 continuous flow automated analysis of seawater nutrients (phosphate, nitrate, nitrite and silicic
38 acid) in the WOCE Hydrographic Program and the Joint Global Ocean Fluxes Study. WHP
39 Operations and Methods. WOCE Hydrographic Program Office, Methods Manual 91-1.
40 November.

- 1 Henson, S.A., Thomas, A.C., 2008. A census of oceanic anticyclonic eddies in the Gulf of Alaska.
2 Deep-Sea Res. I 55, doi:10.1016/j.dsr.2007.11.005.
3
- 4 Hood, E., Scott, D., 2008. Riverine organic matter and nutrients in southeast Alaska
5 affected by glacial coverage. *Nature Geoscience* 1, 583–587.
6
- 7 Hurst, M.P., Bruland, K.W., 2007. An investigation into the exchange of iron and zinc between
8 soluble, colloidal, and particulate size-fractions in shelf waters using low abundance isotopes as
9 tracers in shipboard incubation experiments. *Marine Chemistry*, 103, 211–226.
10
- 11 Hurst, M.P., Aguilar-Islas, A.M., Bruland, K.W., 2010. Iron in the southeastern Bering Sea:
12 elevated leachable particulate Fe in shelf bottom waters as an important source for
13 surface waters. *Continental Shelf Res.* 30, 467–480.
14
- 15 Hutchins, D. A., G. R. DiTullio, Y. Zhang, K. W. Bruland, 1998. An iron limitation mosaic in the
16 California upwelling regime, *Limnol. Oceanogr.*, 43, 1037-1054.
17
- 18 Janout, M. A., Weingartner, T. J., Okkonen, S. R., Whitley, T. E., and Musgrave, D. L., 2009.
19 Some characteristics of Yakutat eddies propagating along the continental slope of the northern
20 Gulf of Alaska, *Deep-Sea Res. II* 56, 2444–2459
- 21 Johnson, K. S., F. P. Chavez, V. A. Elrod, S. E. Fitzwater, J. T. Pennington, K. R. Buck, and P. M.
22 Walz (2001), The annual cycle of iron and the biological response in central California coastal
23 waters, *Geophys. Res. Lett.* 28, 1247– 1250, doi:10.1029/2000GL012433.
- 24 Johnson, W. K., L. A. Miller, N. E. Sutherland, and C. S. Wong (2005), Iron transport by mesoscale
25 Haida eddies in the Gulf of Alaska, *Deep Sea Res. II* 52, 933–953, doi:10.1016/j.dsr2.2004.08.017.
- 26 Johnson, K. S., F. P. Chavez, and G. E. Friederich, Continental-shelf sediment as a primary source
27 of iron for coastal phytoplankton, *Nature* 398, 697-700 1999.
- 28 Ladd, C., Kachel, N. B., Mordy, C. W., Stabeno, P., 2005. Observations from a Yakutat Eddy in
29 the northern Gulf of Alaska. *J. Geophys. Res.* 110, C03003.
- 30 Ladd, C., Mordy, C.W., Kachel, N.B., Stabeno, P.J., 2007. Northern Gulf of Alaska eddies and
31 associated anomalies. *Deep Sea Res. I* 54, 487–509.
- 32 Ladd, C., Cheng, W., 2015. Characteristic of "gap winds" from Cross Sound, Alaska and their
33 effects on regional oceanography. *Deep-Sea Res II* this issue.
- 34 Ladd, C., Cheng, W., Salo, S., 2015. Gap Winds near Kodiak Island, Alaska and effects on regional
35 oceanography. *Deep-Sea Res II* this issue.
- 36 Lam, P. J., Bishop, J. K., Henning, B. C. C., Marcus, M. A., Waychunas, G. A., and Fung, I. Y.
37 2006. Wintertime phytoplankton bloom in the subarctic Pacific supported by continental margin
38 iron. *Global Biogeochem. Cycles*, 20, GB1006, doi:10.1029/2005GB002557.

- 1 Lam, P. J., and Bishop, J. K. B., 2008. The continental margin is a key source of iron to the HNLC
2 North Pacific Ocean. *Geophys. Res. Lett.* 35, 10.1029/2008GL033294
- 3 Landry, M. R. et al., 1997 Iron and grazing constraints on primary production in the central
4 equatorial Pacific: an Eq Pac synthesis. *Limnol. Oceanogr.* 4, 405-418.
- 5 Lippiatt, S. M., Lohan, M. C., and Bruland, K. W., 2010a. The distribution of reactive iron in
6 northern Gulf of Alaska coastal waters. *Mar. Chem.* 121, 187-199.
7
- 8 Lippiatt, S.M., Brown, M.T., Lohan, M.C., Berger, C.J.M., Bruland, K.W., 2010b. Leachable
9 particulate iron in the Columbia River, estuary, and near-field plume. *Estuarine Coastal and Shelf
10 Science* 87, 33–42.
11
- 12 Lippiatt, S. M., Brown, M. T., Lohan, M. C., et al., 2011. Reactive iron delivery to the Gulf of
13 Alaska via a Kenai eddy. *Deep-Sea Res. I* 58, 1091-1102
- 14 Liu, X.W., and Millero, F.J., 2002. The solubility of iron in seawater. *Mar. Chem.* 77, 43-54.
- 15 Maldonado, M. T., and N. M. Price, 2000. Nitrate regulation of Fe reduction and transport by Fe-
16 limited *Thalassiosira oceanica*. *Limnol. Oceanogr.* 45, 814-826.
- 17 Maldonado, M. T., and N. M. Price. 1999. Utilization of iron bound to strong organic ligands by
18 plankton communities in the subarctic Pacific Ocean. *Deep-Sea Res. II* 46: 2447-2473.
- 19 Marchetti, A., Maldonado, M. T., Lane, E. S. and Harrison, P. J., 2006. Iron Requirements of the
20 Pennate Diatom *Pseudo-nitzschia*: Comparison of Oceanic (High-Nitrate, Low-Chlorophyll
21 Waters) and Coastal Species. *Limnol. Oceanogr.* 51, 2092-2101.
22
- 23 Martin, J., Gordon, R., Fitzwater, S., Broenkow, W., 1989. VERTEX: phytoplankton/iron studies in
24 the Gulf of Alaska. *Deep-Sea Res.* 36, 649–680.
- 25 McKay RML, Geider RJ, LaRoche J (1997) Physiological and biochemical response of the
26 photosynthetic apparatus of two marine diatoms to Fe stress. *Plant Physiol.* 114, 615–622.
27
- 28 Menard, H.W., 1979, Holocene Sediment Volume on the Northeast Gulf of Alaska Continental
29 Shelf and Sediment Contribution of Present Day Rivers: US Geol. Survey Marine Geology and
30 Coastal hydrology Pap. 1150, p. 152.
- 31 Milliman, J.D., Syvitski, J.P.M., 1992. Geomorphic/tectonic control of sediment discharge to the
32 ocean: the importance of small mountainous rivers. *Journal of Geology* 100, 525–544.
- 33 Moore, J.K., Doney, S.C., Kleypas, J.A., et al., 2002. An intermediate complexity marine
34 ecosystem model for the global domain. *Deep-Sea Res. II* 49, 403-462.
- 35 Morel, F. M. M., Rueter, J. G., Price, N.M., 1991. Iron nutrition of phytoplankton and its possible
36 importance in the ecology of ocean regions with high nutrient and low biomass, *Oceanography* 4,
37 56-61.

- 1 Morton, P.L., Landing, W.M., Hsu, S.C., Milne, A., Aguilar-Islas, A.M., Baker, A.R., Bowie, A.
2 R., Buck, C.S., Gao, Y., Gichuki, S., Hasings, M., Hatta, M., Johansen, A.M., Losno, R., Mead,
3 C., Patey, M.D., Swarr, Vandermark, G., A., Zamora, L.M., 2013. Methods for the sampling and
4 analysis of marine aerosols: Results from the 2008 GEOTRACES aerosol intercalibration study.
5 *Limnology and Oceanography Methods*. 11: 62-78, doi: 10.4319/lom.2013.11.62.
- 6 Musgrave, D.L., Weingartner, T.J., Royer, T.C., 1992. Circulation and hydrography in the
7 northwestern Gulf of Alaska. *Deep-Sea Research* 39, 1499–1519.
- 8 Peterson, T. D., and Harrison, P. J., 2012. Diatom dynamics in a long-lived mesoscale eddy in the
9 northeast subarctic Pacific Ocean. *Deep-Sea Res. I* 65, 157-170
- 10 Raven, J.A., 1988. The iron and molybdenum use efficiencies of plant growth with different
11 energy, carbon and nitrogen sources. *New Phytologist*, 109, 279–287
12
- 13 Rich, H.W., Morel, F.M.M., 1990. Availability of well-defined iron colloids to the marine diatom
14 *thalassiosira-weisflogii*. *Limnology and Oceanography*, 35, 652–662.
- 15 Rijkenberg, M.J.A., Gerringa, L.J.A., Carolus, V.E., et al., 2006. Enhancement and inhibition of
16 iron photoreduction by individual ligands in open ocean seawater. *Geochim. Cosmochim. Acta*
17 70, 2790-2805.
- 18 Rue, E. L. and K.W. Bruland., 1995. Complexation of Iron (III) by natural organic ligands in the
19 Central North Pacific as determined by a new competitive ligand equilibration/adsorptive
20 cathodic stripping voltammetry method. *Mar. Chem.*, 50, 117-138.
- 21 Schroth A.W., Crusius, J., Hoyer, I., and Campbell R., 2014. Estuarine removal of glacial iron
22 and implications for iron fluxes to the ocean. *Geophys Res. Letters* 41, 3951-3958.
- 23 Stabeno, P.J., et al., 2004. Meteorology and oceanography of the Northern Gulf of Alaska.
24 *Continental Shelf Res.* 24, 859–897.
- 25 Stabeno, P.J., Bond, N.A., Kachel, N.B., Ladd, C., Mordy, C.W., Strom, S.L., 2015. Southeast
26 Alaskan shelf from southern tip of Baranof Island to Kayak Island: Currents, mixing and
27 chlorophyll-a. *Deep-Sea Res II* this issue.
- 28 Strom, S.L., Olson, M.B., Macri, E.L., Mordy, C.W., 2006. Cross-shelf gradients in
29 phytoplankton community structure, nutrient utilization, and growth rate in the coastal Gulf of
30 Alaska. *Mar. Ecol. Prog. Ser.* 328, 75-92.
- 31 Strom S. L., and Fredrickson, K. A., 2015. Spring phytoplankton in the eastern coastal Gulf of
32 Alaska: Photosynthesis and production during high and low bloom years. *Deep-Sea Res II*, this issue.
33
- 34 Sunda, W., Huntsman, S.A., 1995. Iron uptake and growth limitation in oceanic and coastal
35 phytoplankton. *Marine Chemistry* 50, 189–206.

- 1 Waite, J.N., Mueter, F.J., 2013. Spatial and temporal variability of chlorophyll-a concentrations
2 in the coastal Gulf of Alaska, 1998-2011, using cloud-free reconstructions of SeaWiFS and
3 MODIS-Aqua data. *Prog Oceanogr* 116, 179-192.
- 4 Wang, J., Jin, M., Musgrave, D. L., Ikeda, M., 2004. A hydrological digital elevation model for
5 freshwater discharge into the Gulf of Alaska, *J. Geophys. Res.*, 109, C07009,
6 doi:10.1029/2002JC001430.
- 7 Weingartner, T. J., Danielson, S. L., Royer, T. C., 2005. Fresh water variability and
8 predictability in the Alaska Coastal Current. *Deep-Sea Research II* 52, 169–191.
- 9 Wu, J.F., and Boyle, E.A., 1998. Determination of iron in seawater by high-resolution isotope
10 dilution inductively coupled plasma mass spectrometry after Mg(OH)₂ coprecipitation. *Anal.*
11 *Chim. Acta* 367, 183-191.
- 12 Wu, J., 2007. Determination of picomolar iron in seawater by double Mg(OH)₂ precipitation
13 isotope dilution high resolution ICPMS, *Mar. Chem.*, 103, 370– 381.
- 14 Wu, J.F., Aguilar-Islas, A., Rember, R., Weingartner, T., Danielson, S., and Whitley, T., 2009.
15 Size-fractionated iron distribution on the northern Gulf of Alaska. *Geophysical Research Letters*
16 36, L11606.

17
18

19

20

21

- 1 Table 1. Procedurally Defined Fe Fractions. Analyzed fractions are in grey boxes, and calculated
 2 fractions are white boxes

Fe Fraction	Abbreviation	Definition and Notes
<u>Dissolved Fe</u>	<u>D</u> Fe	The fraction that passes through the filter membrane (< 0.4 μm) or filter capsule (< 0.2 μm). Includes colloids and is considered to be available to biology.
Particulate Fe	---	The fraction collected on the filter membrane (> 0.4 μm). It is the sum of LPFe and RPFe
<u>Leachable particulate Fe</u>	LPFe	The particulate fraction that is leached in 2 h with a solution of 25% acetic acid and 0.02 M NH ₂ OH • HCl after a short heating step. This fraction can be mobilized into the dissolved phase over short time scales.
<u>Refractory particulate Fe</u>	RPFe	The particulate fraction that is not leached with the above solution. This fraction is not considered accessible to biology over seasonal time scales.
Reactive Fe	---	The fraction that is potentially available to biology in short timescales (days to weeks). (DFe + LPFe; Lippiat et al., (2010))
<u>Total dissolvable Fe</u>	<u>T</u> DFe	The fraction in an unfiltered sample acidified to pH 1.8. for > 1 month. Includes DFe and is analogous to reactive Fe
Acid-labile particulate Fe	ALPFe	The fraction of particulate Fe that dissolves when an unfiltered sample is acidified to pH 1.8 (TDFe – DFe). It is analogous to LPFe.
Labile particulate Fe	---	Either LPFe or ALPFe

3

4

1 Table 2. Sampling Season, Location and Method

Sampling Season	Sampling Location	Sampling Method	Measured (Derived) Fe Fraction
<u>Spring</u>	<u>Southeast GoA Profiles at SEA, SEG, and YBC</u>	UAF Vanes	DFe, LPFe, RPFe (PFe, Reactive Fe)
	Southeast GoA Surface Samples	Towed Fish	DFe, TDFe (ALPFe)
<u>Late Summer</u>	Western GoA surface samples along Seward Line, PWS	Towed Fish	DFe, TDFe (ALPFe)

2

3

1

2 Table 3. Organic Speciation of DFe .

Sample	[L ₁] (nM)	log K ₁	[L ₂] (nM)	log K ₂	[L ₃] (nM)	log K ₃	[eL ₁] (nM)	[L _{total}] (nM)	[eL _{tot}] (nM)
Spring ~ 1 m									
T01-01 (ChS)	2.73	13.00	0.42	11.84			0.31	3.15	0.73
T01-02 (ChS)	2.60	12.38	0.66	11.45			0.40	3.26	1.06
T02-01 (CS)	3.12	12.67	0.76	11.47			0.23	3.88	0.99
T02-03 (CS)	3.65	12.68	0.29	11.85			0.32	3.94	0.62
T02-05 (CS)	2.59	12.27	1.21	11.25			0.65	3.80	1.85
T03-03 (KIs)	1.92	12.71	1.19	11.17			0.55	3.10	1.73
T03-07 (KIs)	1.41	12.17	0.34	11.26			0.49	1.74	0.83
T04-08* (KIs)	3.78	12.36	0.47	11.97			0.81	4.25	1.28
T05-03 (YBC)	1.17	12.16	1.05	11.37			0.67	2.22	1.72
T07-09 (ChS)	1.57	12.80	0.54	11.40			0.42	2.11	0.96
Spring 20 m									
YBC-10	1.36	12.15	0.70	11.53			0.65	2.06	1.34
YBC-40			1.38	11.92	1.36	10.82	---	2.74	1.95
YBC-50+			2.76	11.66			---	2.76	1.94
SEA 20			1.74	11.40			---	1.74	1.19
SEG 0	1.00	12.05	0.50	11.41			0.46	1.50	0.96
SEG 0a			0.79	11.57	0.85	10.65	---	1.64	1.16
SEG 20a	1.18	12.04			4.14	10.38	0.67	5.32	4.81
Late Summer ~1 m									
GAK 5	1.43	12.14	0.54	11.44			1.00	1.97	1.54
GAK 9					1.39	10.93	---	1.39	1.16
GAK 10	0.70	12.39	0.41	11.31			0.39	1.11	0.81
GAK 13			0.74	11.67	0.96	10.73	---	1.70	1.65
GAK 5	0.35	12.01			2.91	10.23	0.20	3.26	3.11
GAK 1	5.97	12.30	1.06	11.63			1.11	7.03	2.17

3 Ligand concentrations and conditional stability constants are reported as the average of the results from two interpretation
4 techniques applied to the data from each sample. Ligand classes (L₁, L₂, L₃) defined by conditional stability constants (log
5 $K_{FeL_i, Fe}^{cond}$; abbreviated as log K_i for i = 1, 2, 3), where L₁: log K₁ = > 12, L₂: log K₂ = 11 – 12, L₃: log K₃ = 10 – 11. Excess L₁
6 ([eL₁]) and excess total ligand ([eL_{tot}]) concentrations calculated from subtracting ambient dissolved iron concentrations from L₁
7 ([L₁]) and total ligand ([L_{tot}] = [L₁] + [L₂] + [L₃]) concentrations, respectively.

8 * Suspected contamination during sample collection

1 **Table 4. Nutrient relationships**

Cruise	Sample	Longitude [deg_east]	Latitude [deg_north]	Depth [m]	DFe [nM]	N+N [umol/kg]	Fe(ex) [nM]	Fe:C [umol:mol]
1TT11	T01-01	-134.79	56.19	Surface	2.41	--	--	--
1TT11	T01-02	-134.89	56.26	Surface	2.21	--	--	--
1TT11	T01-03	-134.97	56.32	Surface	1.36	--	--	--
1TT11	T02_01	-137.68	58.23	Surface	2.89	11.65	-0.97	50
1TT11	T02_02	-137.84	58.32	Surface	3.74	12.08	-0.26	50
1TT11	T02_03	-137.91	58.37	Surface	3.32	10.80	-0.25	50
1TT11	T02_04	-137.98	58.41	Surface	1.83	11.05	-1.83	50
1TT11	T02_05	-138.05	58.46	Surface	1.94	11.24	-1.78	50
1TT11	T03_01	-141.36	59.68	Surface	2.77	--	--	--
1TT11	T03_02	-141.64	59.66	Surface	1.25	--	--	--
1TT11	T03_03	-142.78	59.61	Surface	1.37	--	--	--
1TT11	T03_04	-143.01	59.60	Surface	(>10)*	6.23	--	--
1TT11	T03_05	-143.20	59.59	Surface	1.41	5.41	-0.38	50
1TT11	T03_06	-143.39	59.58	Surface	1.52	5.57	-0.33	50
1TT11	T03_07	-143.58	59.57	Surface	0.91	6.85	-1.36	50
1TT11	T03_08	-143.83	59.55	Surface	0.98	6.72	-1.25	50
1TT11	T04_01	-145.00	59.74	Surface	4.50	4.73	2.93	50
1TT11	T04_02	-145.16	59.74	Surface	(>10)*	0.30	--	--
1TT11	T04_03	-145.32	59.74	Surface	1.23	0.21	1.16	50
1TT11	T04_04	-145.42	59.70	Surface	1.84	0.18	1.78	50
1TT11	T04_05	-145.43	59.63	Surface	1.67	0.21	1.60	50
1TT11	T04_06	-145.42	59.58	Surface	0.76	7.71	-1.80	50
1TT11	T04_07	-145.43	59.51	Surface	0.59	8.06	-2.08	50
1TT11	T04_08	-145.42	59.39	Surface	(2.97)*	7.98	0.33	50
1TT11	T04_09	-145.44	59.31	Surface	1.70	8.06	-0.97	50
1TT11	T05_01	-145.12	59.25	Surface	1.14	0.27	1.05	50
1TT11	T05_02	-141.15	58.62	Surface	0.35	8.57	-2.49	50
1TT11	T05_03	-140.82	58.58	Surface	0.49	8.12	-2.20	50
1TT11	T05_04	-140.35	58.52	Surface	0.28	8.69	-2.60	50
1TT11	T05_05	-139.84	58.44	Surface	0.44	8.58	-2.40	50
1TT11	T05_06	-139.40	58.37	Surface	1.50	8.48	-1.31	50
1TT11	T05_07	-138.92	58.27	Surface	1.94	9.80	-1.31	50
1TT11	T05_08	-138.43	58.20	Surface	0.94	9.65	-2.26	50
1TT11	T05_09	-137.92	58.14	Surface	4.91	10.28	1.51	50
1TT11	T05_10	-137.62	58.11	Surface	0.63	8.89	-2.31	50
1TT11	T06_01	-136.96	57.85	Surface	1.12	4.66	-0.42	50
1TT11	T06_02	-137.12	57.81	Surface	0.97	0.24	0.89	50
1TT11	T06_04	-137.03	57.62	Surface	1.51	0.22	1.44	50
1TT11	T06_05	-136.89	57.48	Surface	0.57	1.40	0.10	50

1TT11	T06_06	-136.78	57.38	Surface	0.35	7.76	-2.22	50
1TT11	T06_07	-136.66	57.26	Surface	0.78	8.44	-2.01	50
1TT11	T07_01	-135.69	56.77	Surface	1.34	2.64	0.46	50
1TT11	T07_02	-135.64	56.69	Surface	2.33	4.41	0.87	50
1TT11	T07_03	-135.58	56.61	Surface	0.77	8.69	-2.11	50
1TT11	T07_04	-135.52	56.52	Surface	1.32	8.01	-1.33	50
1TT11	T07_05	-135.45	56.43	Surface	0.76	8.89	-2.19	50
1TT11	T07_06	-135.38	56.33	Surface	0.94	11.31	-2.80	50
1TT11	T07_07	-135.29	56.20	Surface	0.87	10.04	-2.46	50
1TT11	T07_08	-135.21	56.11	Surface	0.99	11.44	-2.80	50
1TT11	T07_09	-135.15	56.02	Surface	1.15	12.27	-2.91	50
2Tx11	PWS0	-147.82	60.52	Surface	4.61	0.33	4.57	20
2Tx11	GAK4	-149.06	59.41	Surface	0.36	6.70	-0.53	20
2Tx11	GAK4.5	-149.00	59.35	Surface	0.55	7.10	-0.40	20
2Tx11	GAK5	-148.94	59.29	Surface	0.43	6.01	-0.37	20
2Tx11	GAK5.5	-148.86	59.20	Surface	0.55	6.30	-0.28	20
2Tx11	GAK6	-148.79	59.13	Surface	0.92	4.12	0.37	20
2Tx11	GAK6.5	-148.70	59.01	Surface	0.37	4.42	-0.22	20
2Tx11	GAK7	-148.65	58.97	Surface	0.46	3.97	-0.07	20
2Tx11	GAK7.5	-148.59	58.90	Surface	0.41	3.32	-0.03	20
2Tx11	GAK1	-149.47	59.87	Surface	4.87	2.29	4.56	20
2Tx11	GAK2	-149.31	59.68	Surface	1.56	3.66	1.08	20
2Tx11	GAK3	-149.20	59.58	Surface	3.27	2.93	2.89	20
2Tx11	GAK4	-149.05	59.43	Surface	1.70	3.78	1.19	20
2Tx11	GAK5	-148.90	59.28	Surface	0.15	3.78	-0.35	20
2Tx11	GAK6	-148.77	59.14	Surface	0.40	3.52	-0.07	20
2Tx11	GAK7	-148.63	58.95	Surface	0.21	3.15	-0.21	20
2Tx11	GAK8	-148.49	58.80	Surface	0.25	3.93	-0.27	20
2Tx11	GAK9	-148.36	58.69	Surface	0.23	3.03	-0.17	20
2Tx11	GAK10	-148.17	58.49	Surface	0.30	2.02	0.04	20
2Tx11	GAK11	-148.04	58.36	Surface	0.25	2.22	-0.04	20
2Tx11	GAK12	-147.91	58.21	Surface	0.20	1.27	0.03	20
2Tx11	GAK13	-147.80	58.11	Surface	0.05	9.92	-1.26	20
1TT11	sea20	224.31	56.31	20.00	0.55	11.67	-3.31	50
1TT11	seg0	223.92	57.37	20.00	0.92	11.62	-2.93	50
1TT11	seg0	223.92	57.37	40.00	0.54	13.51	-3.94	50
1TT11	seg0	223.92	57.37	60.00	1.29	13.56	-3.20	50
1TT11	seg20	223.37	57.20	50.00	0.51	11.84	-3.41	50
1TT11	seg20	223.37	57.20	300.00	1.17	35.53	-10.60	50
1TT11	ybc50f	218.93	58.78	20.00	0.82	9.11	-2.20	50
1TT11	ybc50f	218.93	58.78	50.00	0.30	12.24	-3.76	50
1TT11	ybc40	219.38	58.94	20.00	0.79	9.12	-2.23	50
1TT11	ybc40	219.38	58.94	50.00	0.89	14.72	-3.99	50

1TT11	ybc40	219.38	58.94	75.00	2.12	18.89	-4.14	50
1TT11	ybc10	219.94	59.34	20.00	0.71	10.01	-2.60	50
1TT11	ybc10	219.94	59.34	50.00	0.65	13.55	-3.84	50
1TT11	ybc10	219.94	59.34	75.00	0.83	14.90	-4.11	50
1TT11	seg20a	223.40	57.20	20.00	0.51	13.38	-3.92	50
1TT11	seg20a	223.40	57.20	50.00	0.99	19.53	-5.48	50
1TT11	seg20a	223.40	57.20	75.00	0.61	19.90	-5.98	50
1TT11	seg20a	223.40	57.20	100.00	0.51	13.66	-4.01	50

1

2 * Suspected contamination during sample collection

3

1 **Figure Captions**

2 Fig. 1. Map showing the general surface circulation of the Gulf of Alaska, and locations sampled
3 for Fe and related parameters. White circles indicate locations where surface transects were
4 sampled. Black circles show stations where Fe profiles were collected. Heavy outlines on circles
5 denote locations where Fe-binding organic ligand samples were collected. The Alaska Coastal
6 Current is indicated by thin black arrows. Also labeled are Prince William Sound (PWS), Kayak
7 Island (K Is), Yakutat Bay (Y Bay), Cross Sound (CS), Chatham Strait (ChS), the mouths of the
8 Copper River (Copper R) and Alsek River (Alsek R). The 250 m contour line denotes the shelf
9 break.

10 Fig 2. Map of surface transects during spring 2011 along the southeast GoA shelf. Temperature
11 (a), salinity (b), and fluorescence (c) were obtained from the ship's underway system. Samples
12 for the analysis of nitrate plus nitrite (N+N) (d), DFe (e), and TDFe (f) were obtained from with
13 a trace-metal-clean towed sampler. Kayak Island (K Is), Yakutat Bay (Y Bay), Cross Sound (CS)
14 and Chatham Strait (ChS) are indicated along with the 250 m isobath.

15 Fig 3. Depth profiles at Station SEA5, located 5 km from shore, and SEA 20, located 20 km from
16 shore. Temperature (a, c), salinity (a, c), % beam transmission (% Beam c) (b, d), and factory
17 calibrated Chl a (b, d) were collected from sensors on the ship's CTD rosette, and DFe (a, c),
18 LPFe (b,d) and RPFfe (b, d) were collected from UAF vanes deployed above the CTD rosette.

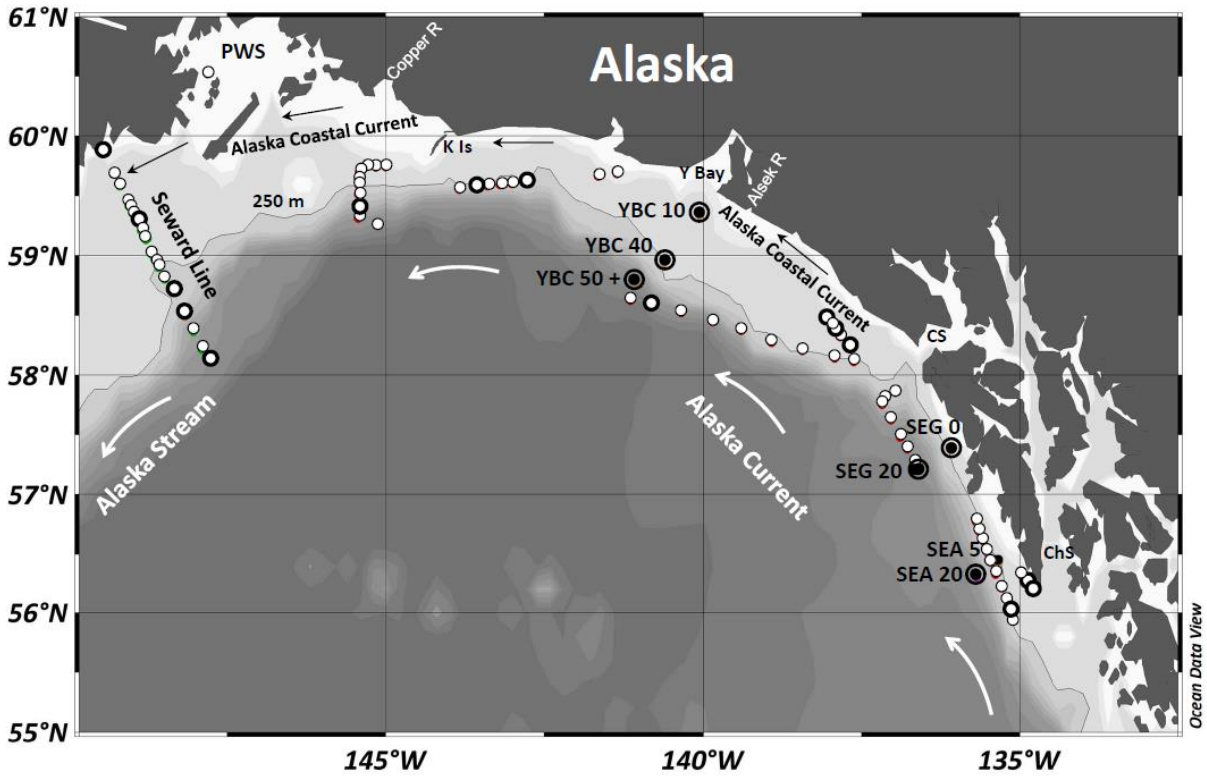
19 Fig 4. Depth profiles from 7 May at Station SEG0, located < 1 km from shore, and SEG20,
20 located 20 km from shore. Temperature (a, c), salinity (a, c), % beam transmission (% Beam c)
21 (b, d), and factory calibrated Chl a (b, d) were collected from sensors on the ship's CTD rosette,
22 and DFe (a, c), LPFe (b,d) and RPFfe (b, d) were collected from UAF vanes deployed above the
23 CTD rosette.

24 Fig 5. Depth profiles from 17 May at Station SEG0, located < 1 km from shore, and SEG20,
25 located 20 km from shore. Temperature (a, c), salinity (a, c), % beam transmission (% Beam c)
26 (b, d), and factory calibrated Chl a (b, d) were collected from sensors on the ship's CTD rosette,
27 and DFe (a, c), LPFe (b,d) and RPFfe (b, d) were collected from UAF vanes deployed above the
28 CTD rosette.

29 Fig 6. Depth profiles at Station YBC10, located 10 km from shore, YBC40, located 40 km from
30 shore, and YBC50+, located > 50 km from shore. Temperature (a, c, e), salinity (a, c, e), % beam
31 transmission (% Beam c) (b, d, f), and Chl a (b, d, f) were collected from the ship's CTD rosette,
32 and DFe (a, c, e), LPFe (b, d, f) and RPFfe (b, d, f) were collected from UAF vanes deployed
33 above the CTD rosette.

34 Fig 7. Consolidated depth profiles at Stations SEA, SEG and YBC. DFe (a, d), LPFe (b, e), and
35 RPFfe (c, f) collected from UAF vanes deployed starting 10 m above the CTD rosette.

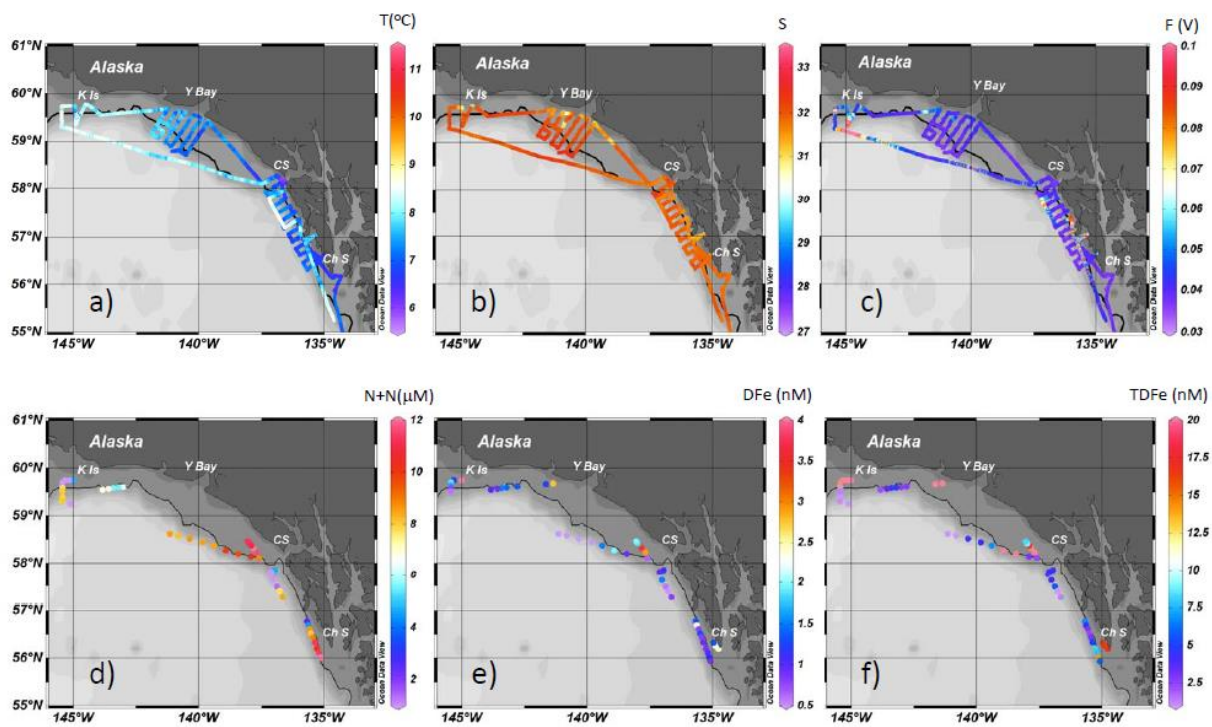
- 1 Fig. 8. Surface data during 16, 17, and 19 September 2011 along the Seward Line. a)
2 Temperature and N+N, b) Salinity and DFe, and c) TDFe and the % of reactive Fe in the
3 dissolved phase (% DFe).
- 4 Fig. 9. Scatterplot of DFe as a function of reactive Fe (TDFe or LPFe+DFe). Vertical dash line
5 marks 50 nM reactive Fe. Samples from this study (2011) were collected from the surface tow
6 fish during spring (white circles) and late summer (black triangles); samples from 2007 obtained
7 from Lippiatt et al. (2010a) and were also obtained with a surface tow fish.
- 8 Fig. 10. Scatterplot of DFe as a function of strong-Fe binding ligand concentrations [L_1]. The
9 dash line denotes the 1:1 line. Data is from 2011 samples collected from the surface tow fish in
10 spring (grey circles) and summer (black circles), and from UAF vanes position at 20 m (white
11 triangles).
- 12 Fig. 11. Variability in DFe as a function of salinity along the Seward Line. Samples were
13 collected from GAK 1 to GAK 13 during this study (2011; black circles), 2007 (grey squares;
14 Lippiatt et al., 2010a), and 2004 (white diamonds; Wu et al., 2009)
- 15



1

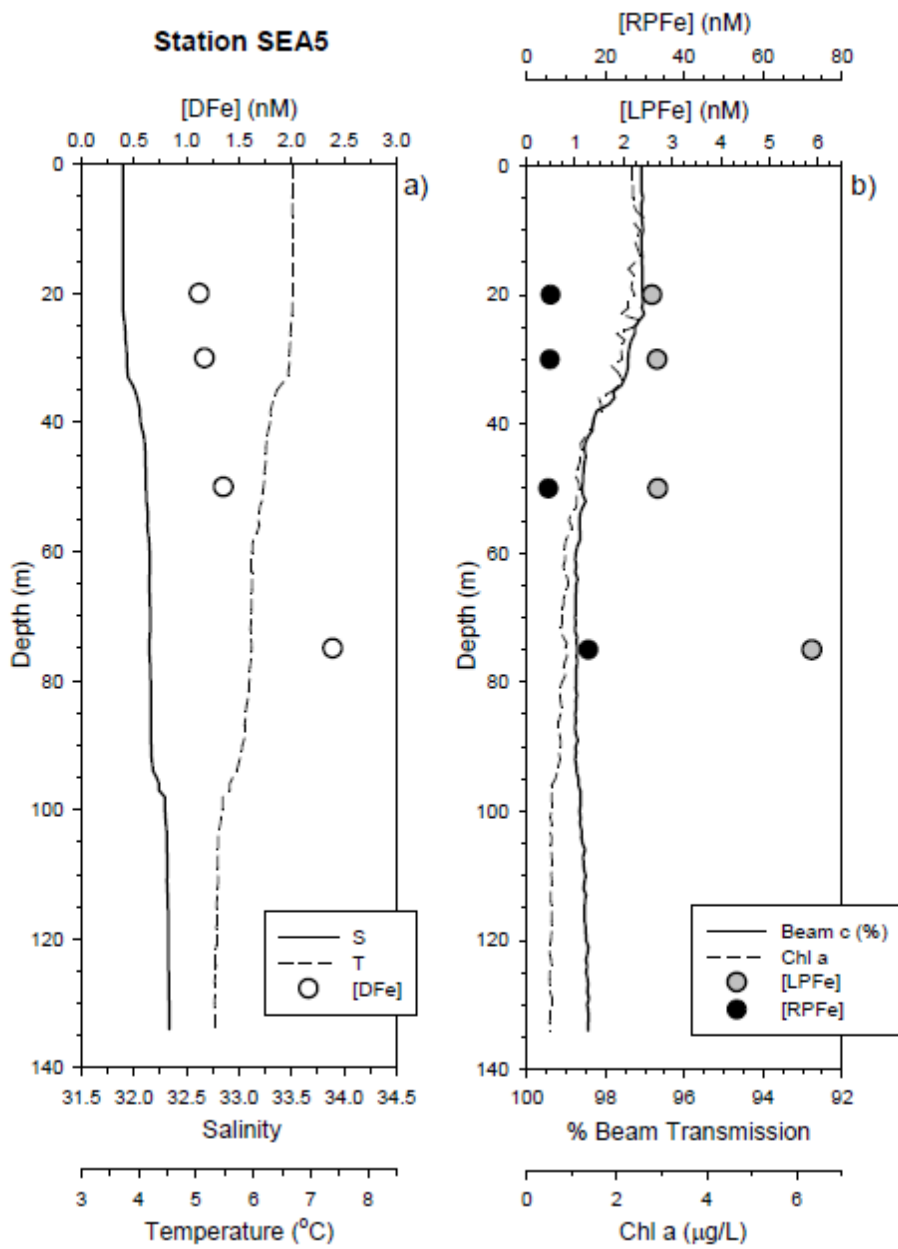
2 Figure 1

3



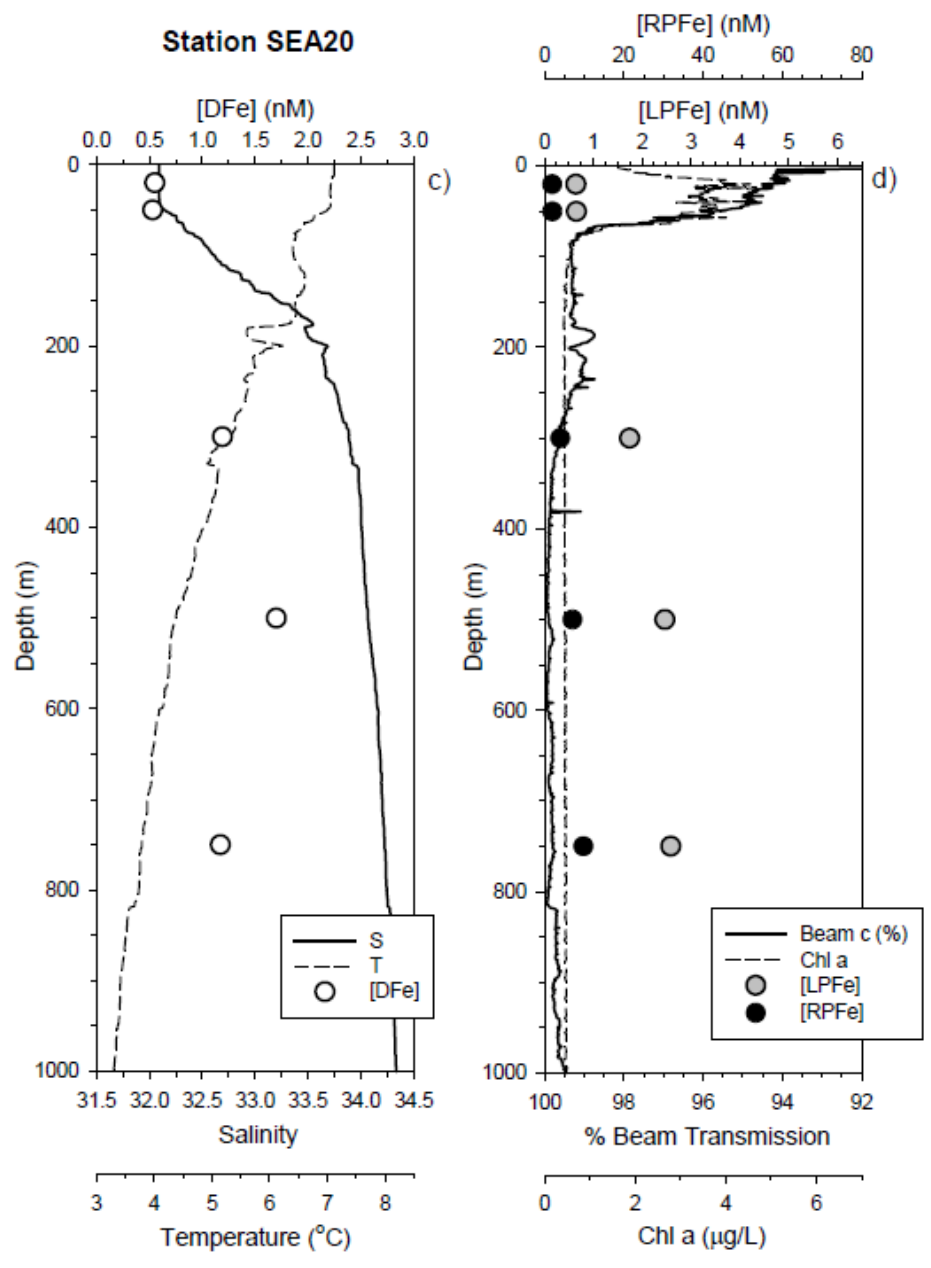
1

2 Figure 2



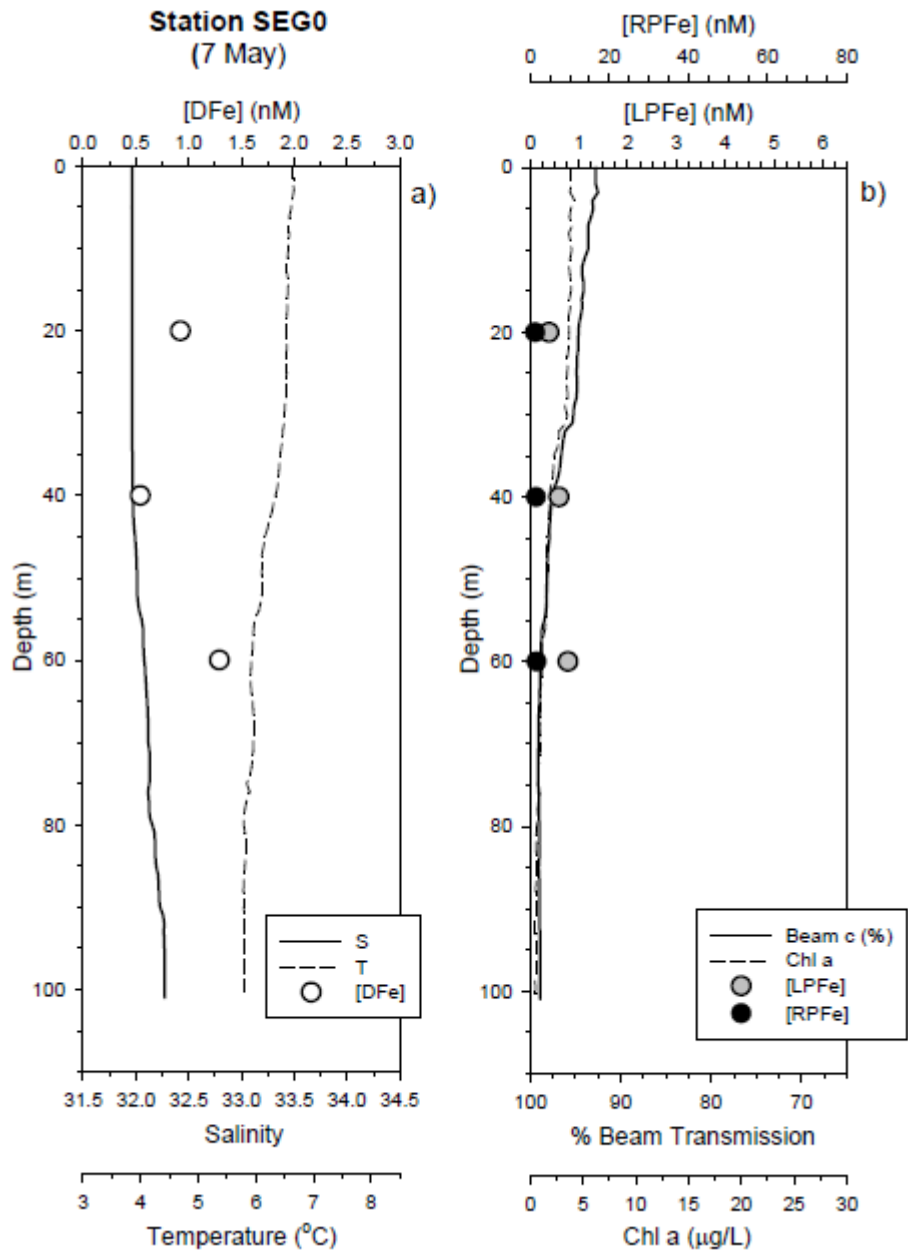
1

2 Figure 3 a-b



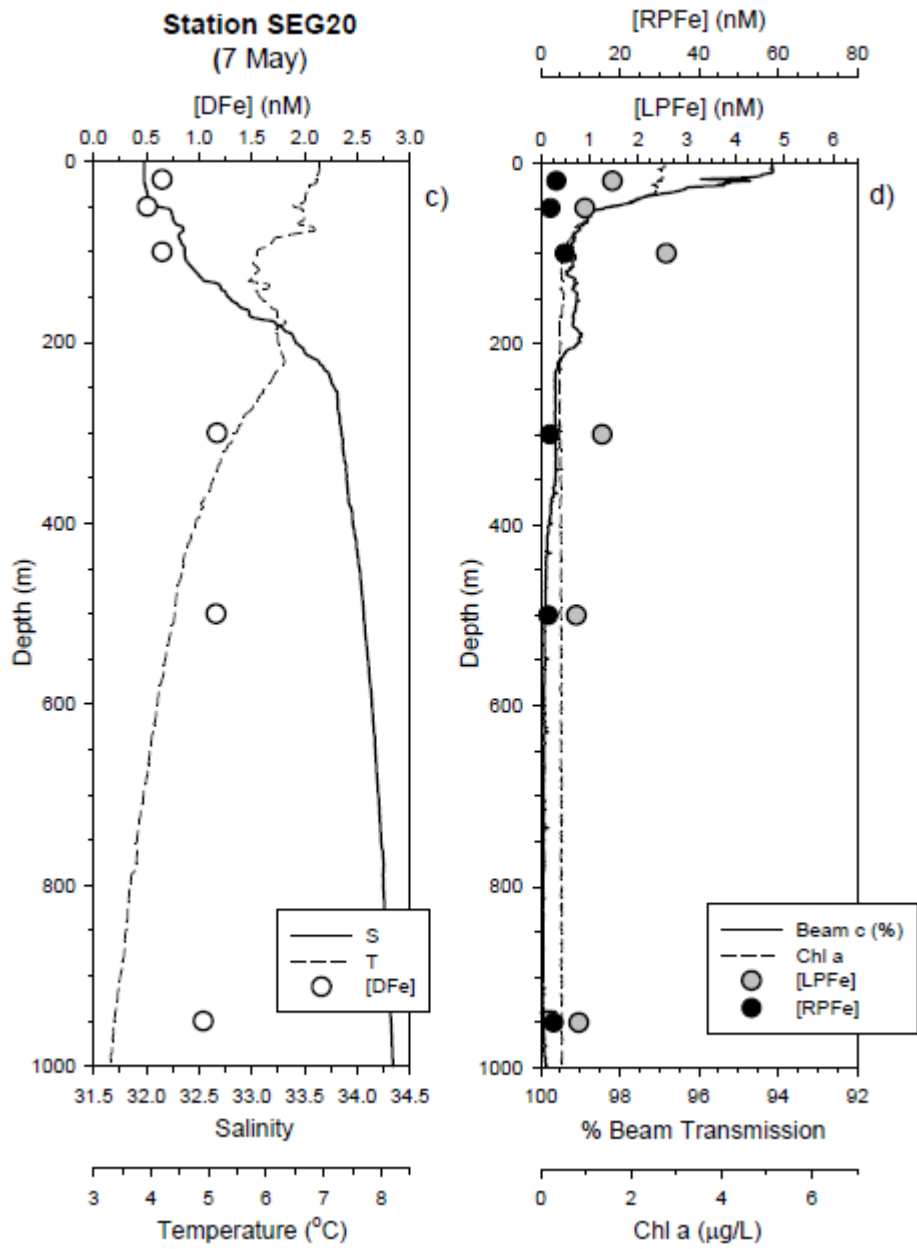
1

2 Figure 3 c-d



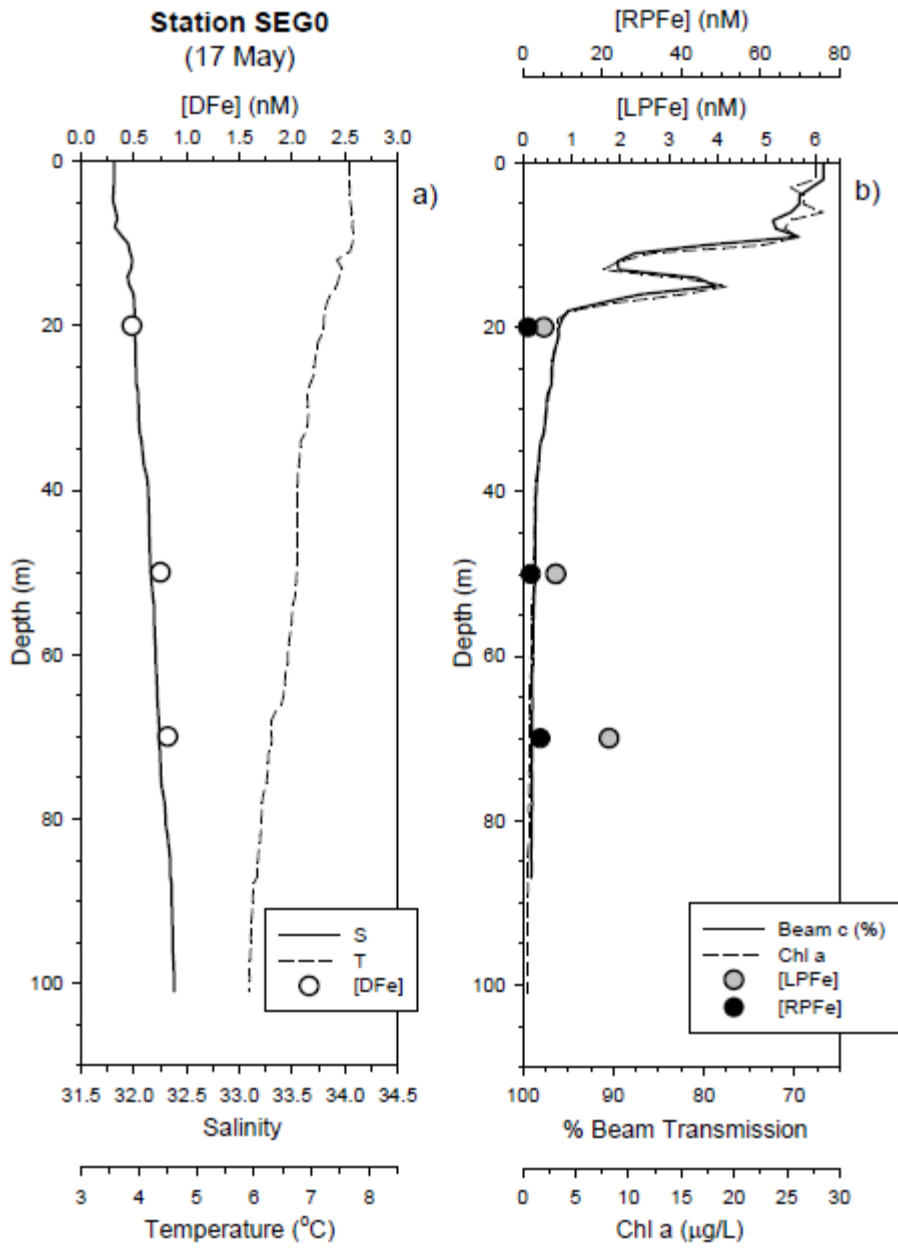
1

2 Figure 4 a-b

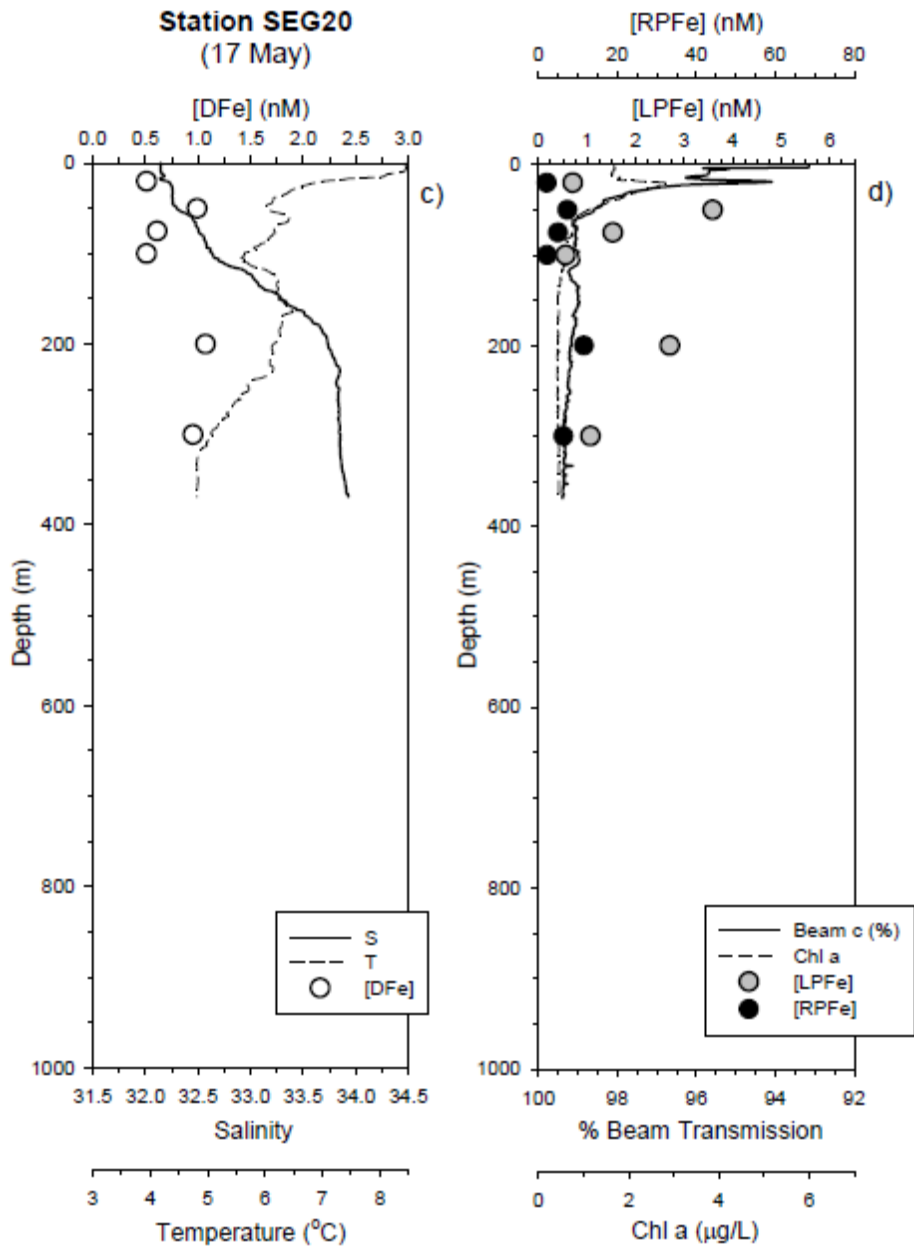


1

2 Figure 4 c-d

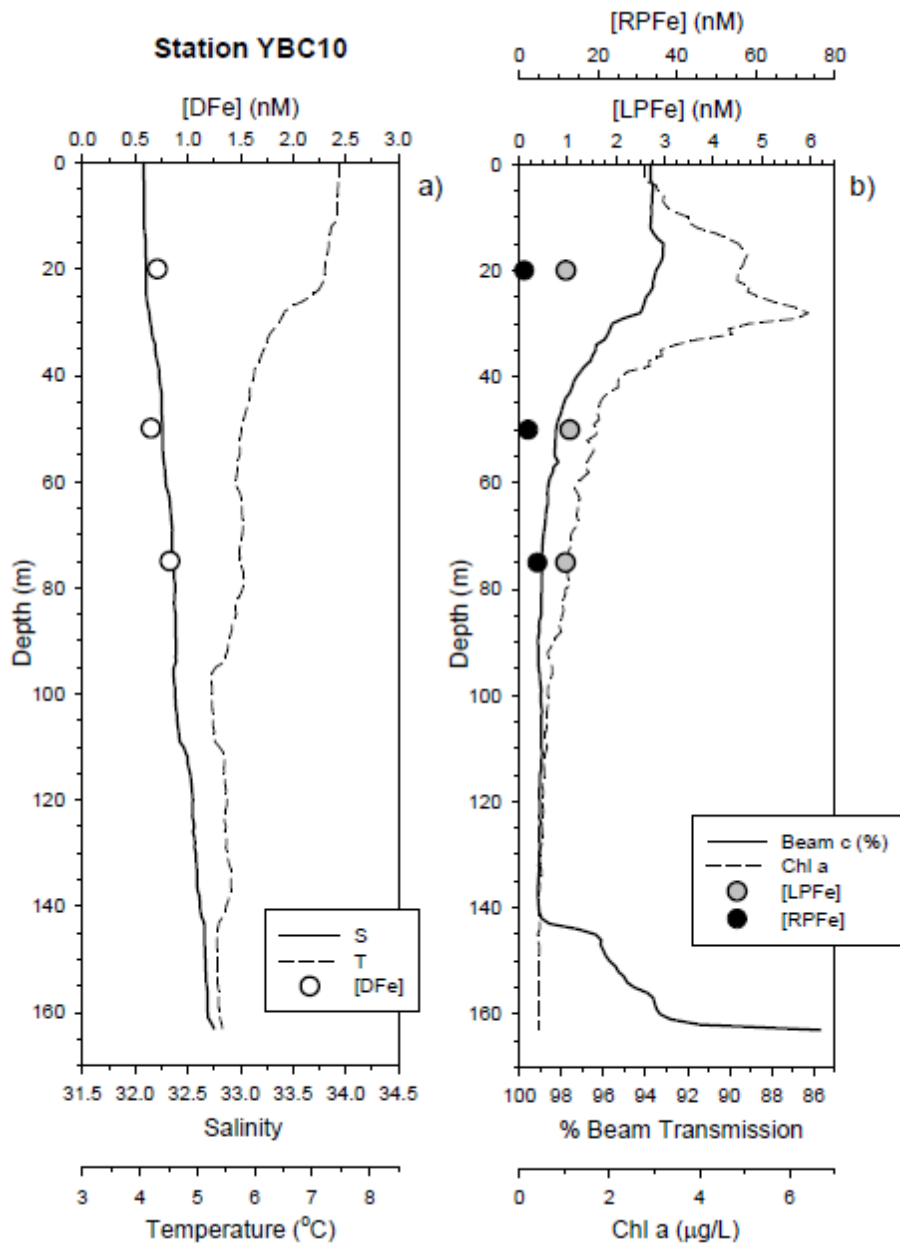


1
2 Figure 5 a-b



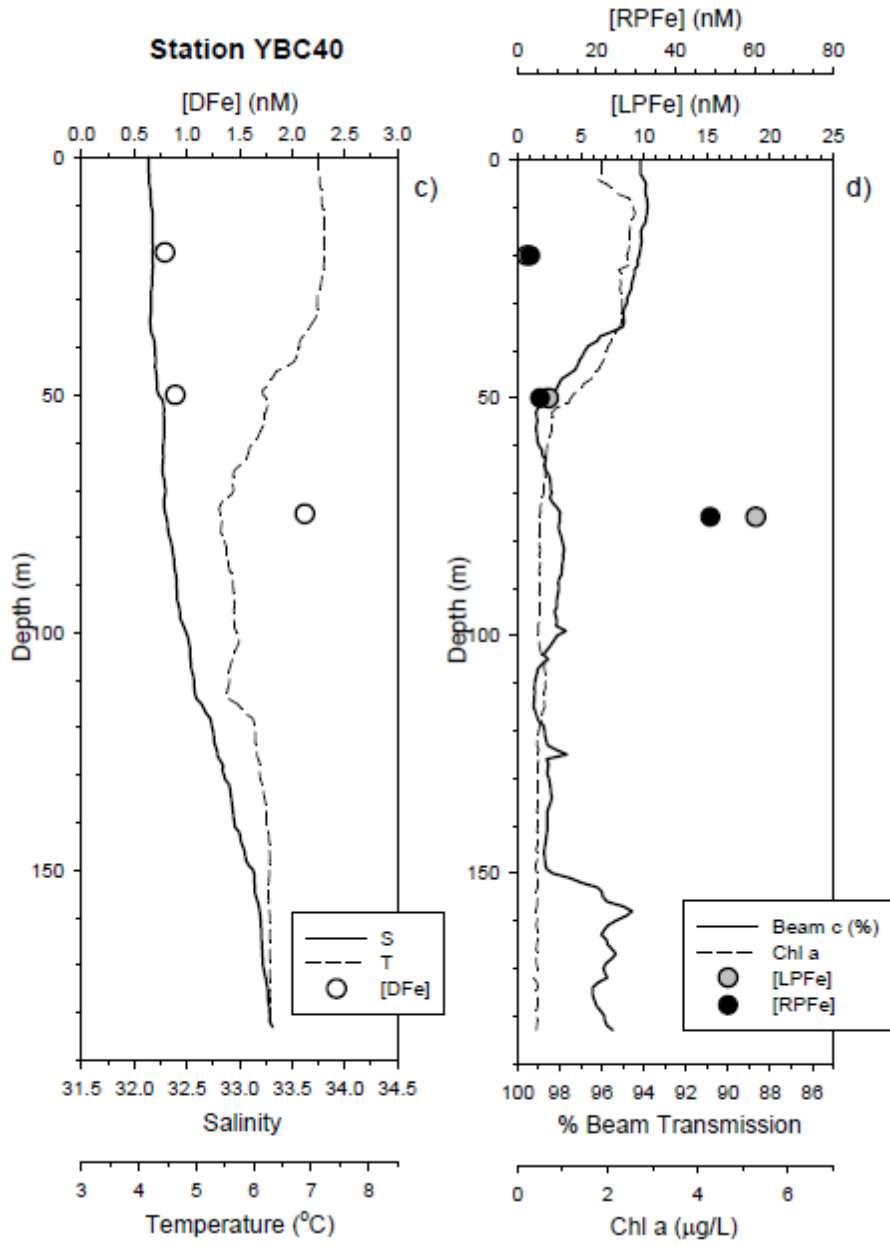
1

2 Figure 5 c-d



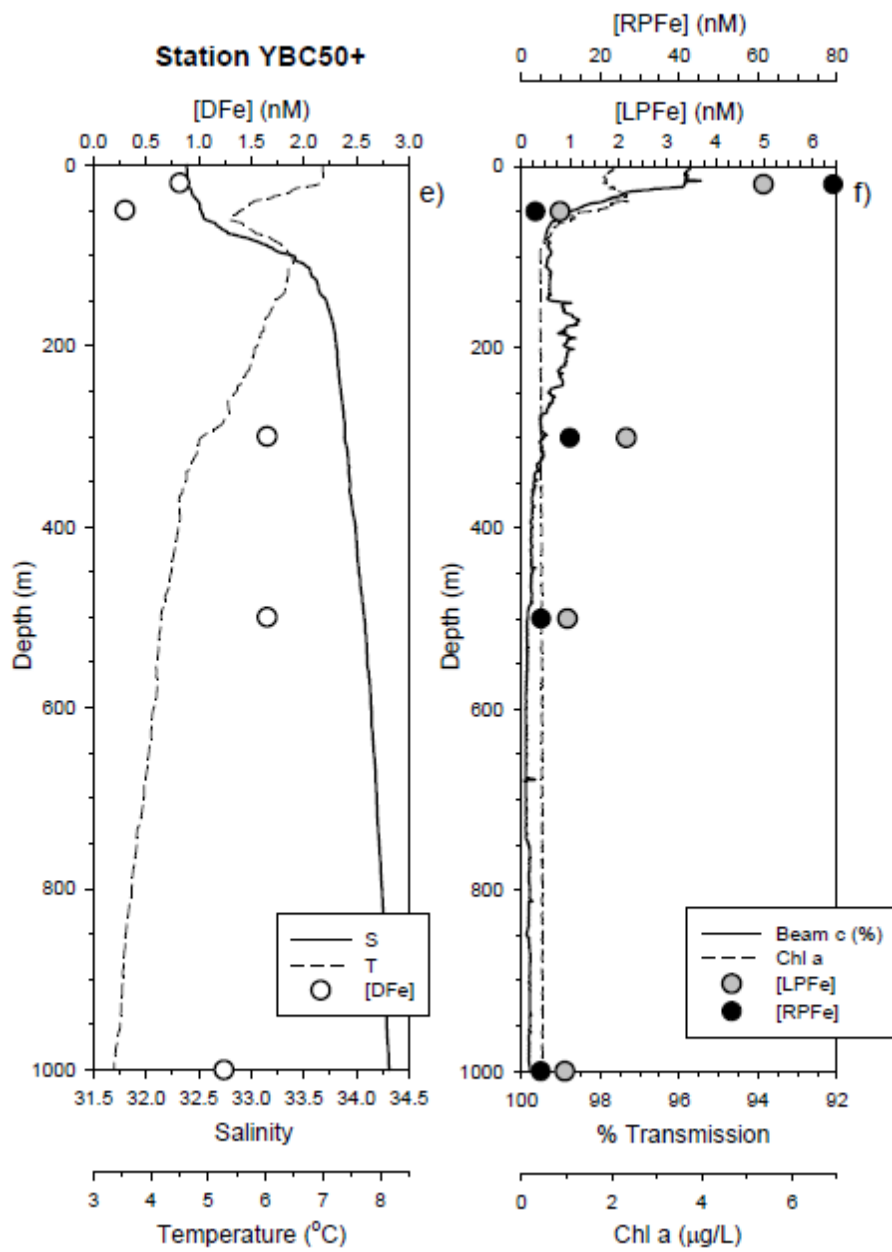
1

2 Figure 6 a-b



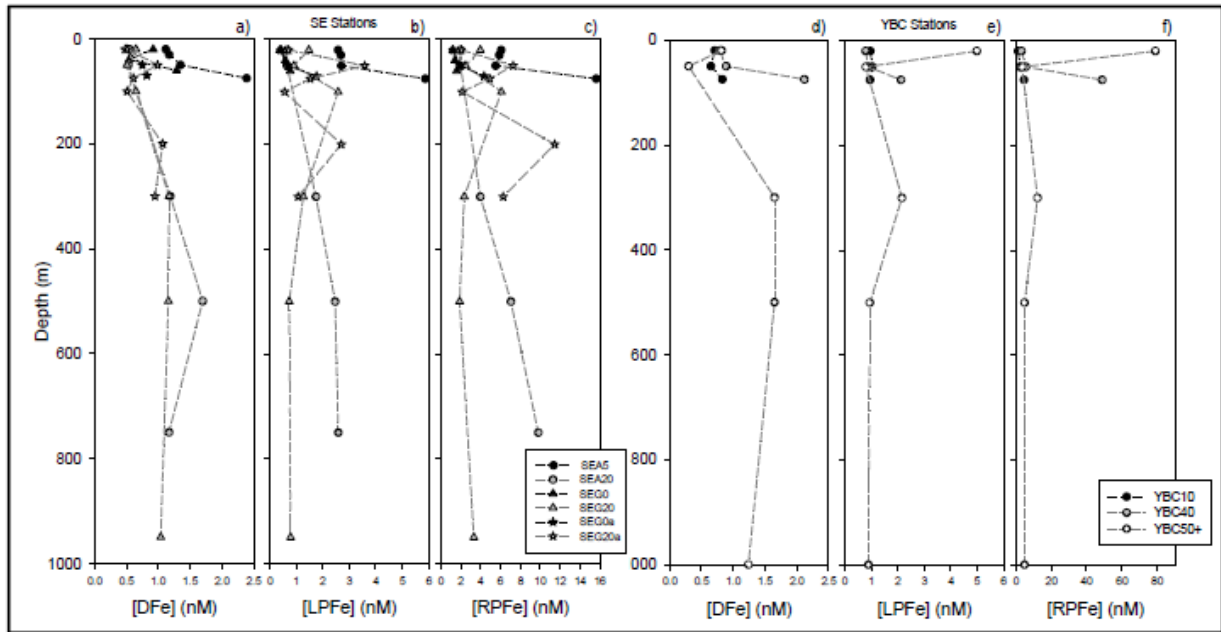
1

2 Figure 6 c-d



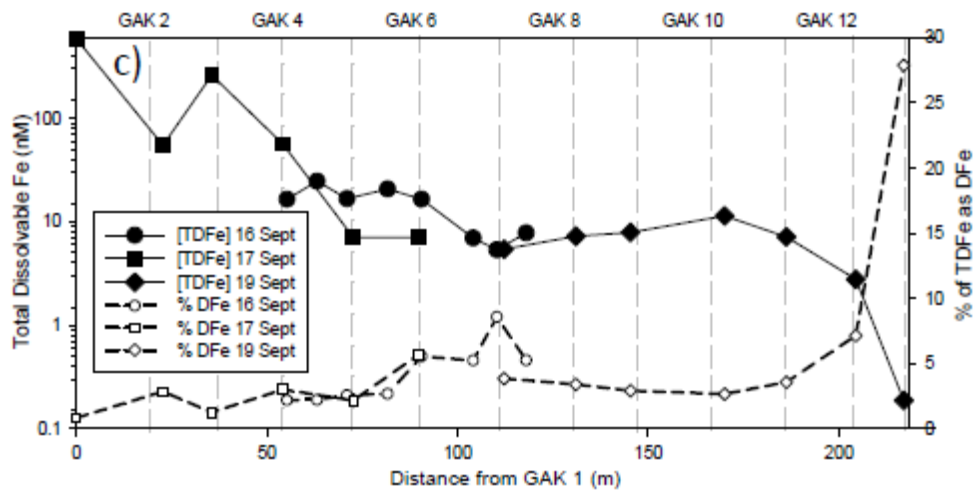
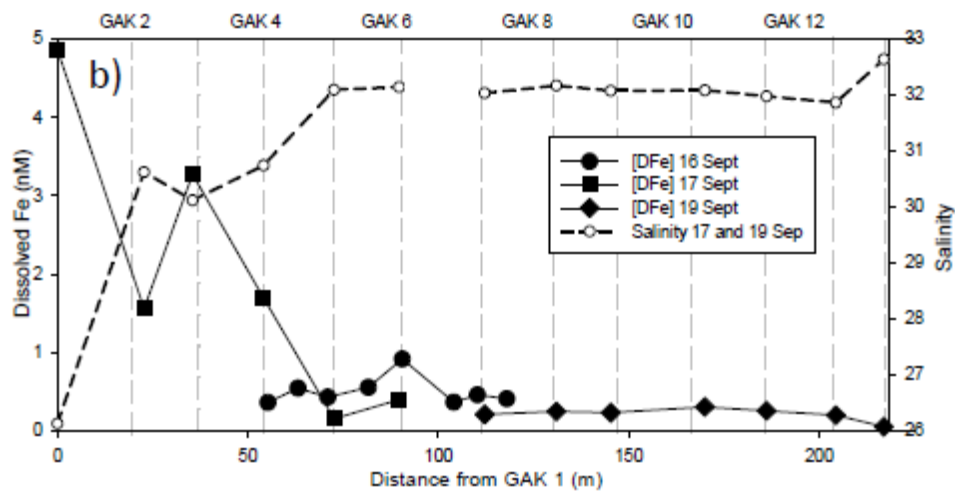
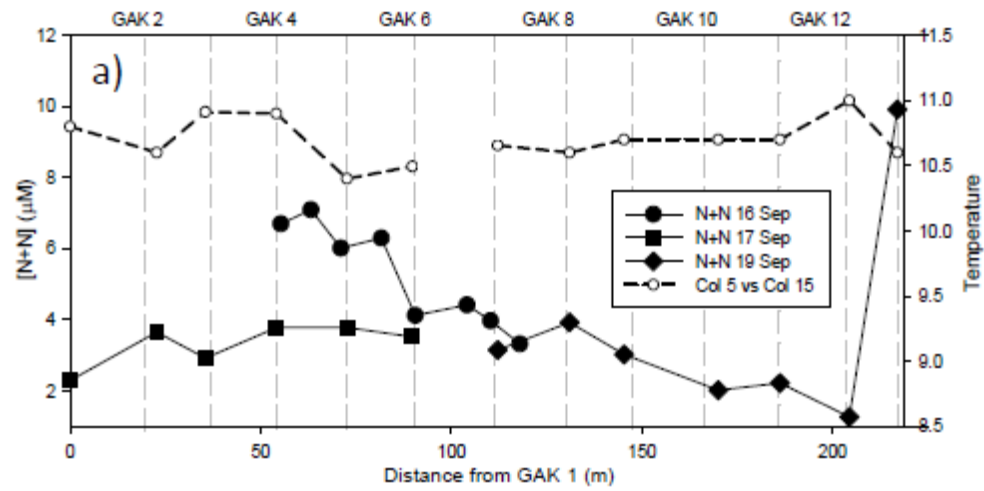
1

2 Figure 6 e-f



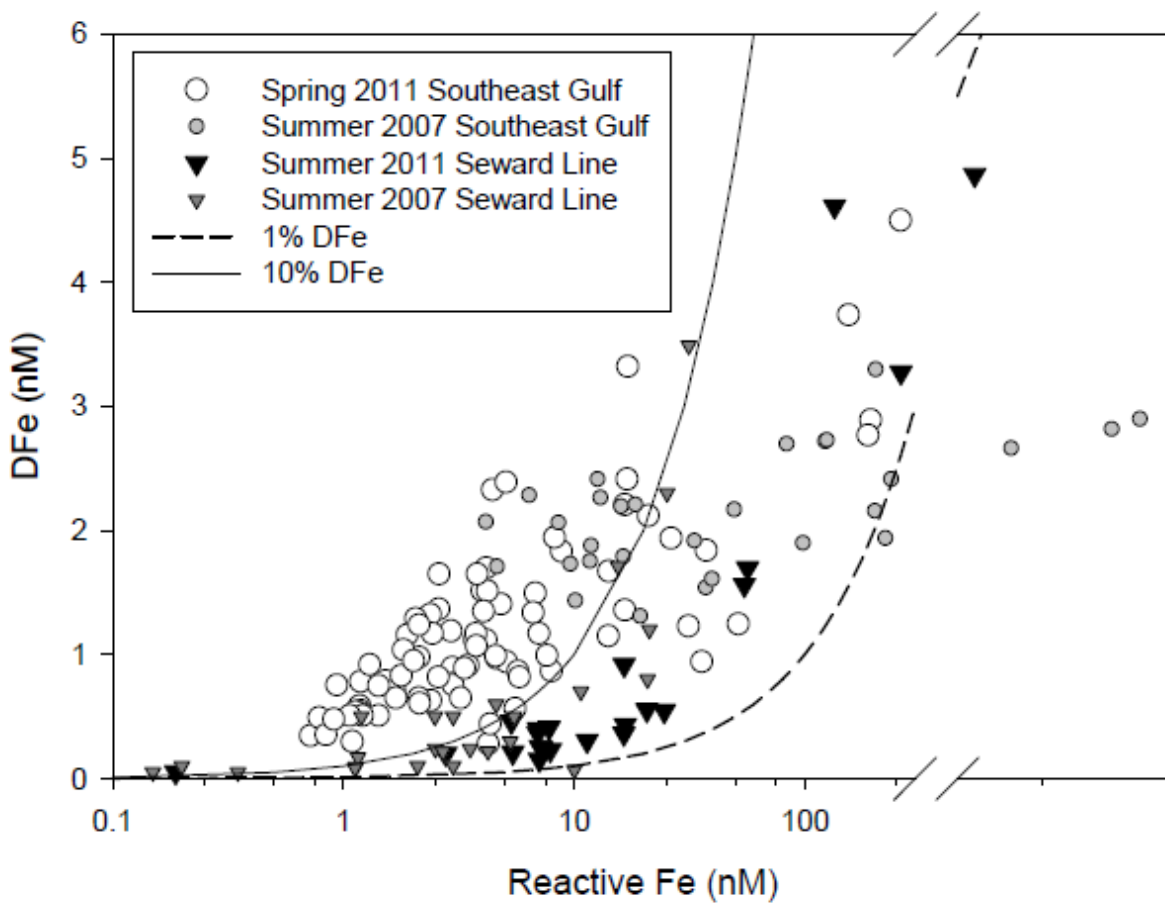
1

2 Figure 7



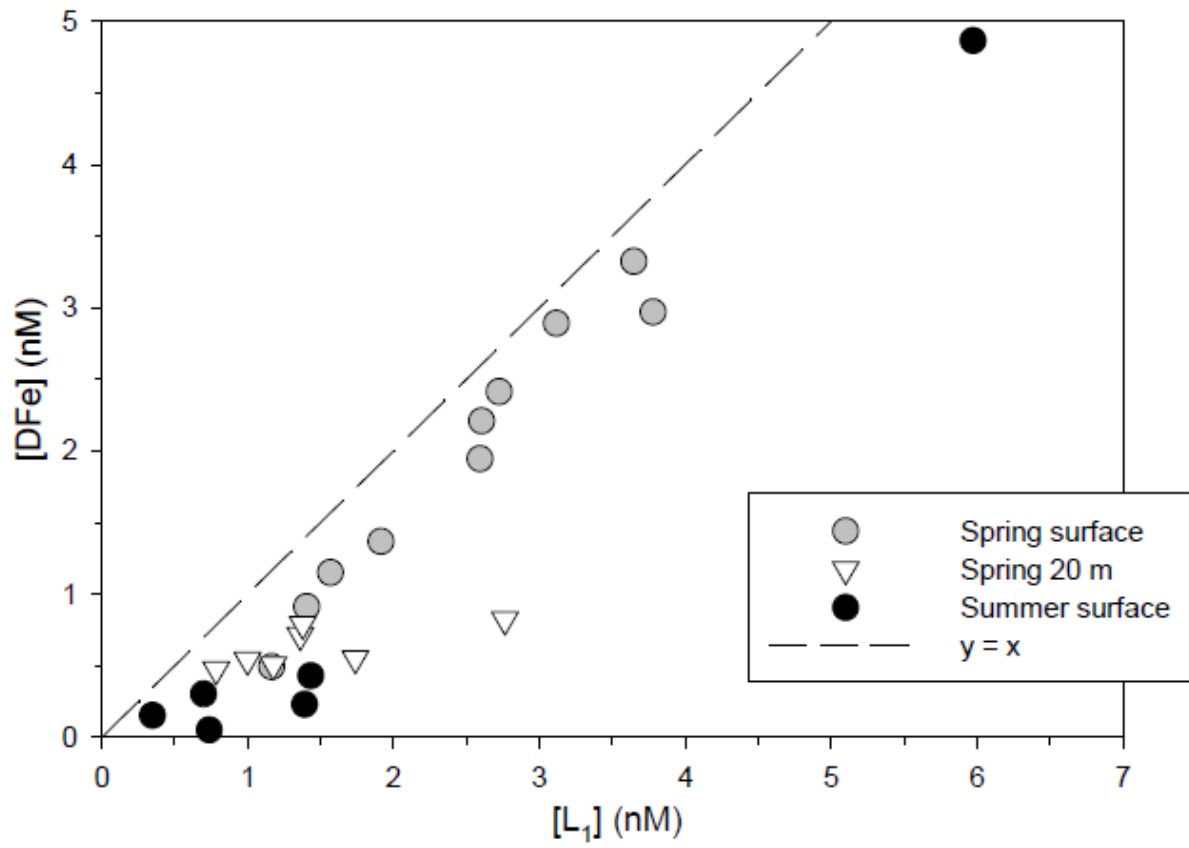
1

2 Figure 8



1

2 Figure 9



1

2 Figure 10

